PADUA UNIVERSITY, IMAGE DEPARTMENT

BOSTON UNIVERSITY, DEPARTMENT OF THE EARTH SCIENCES

MODELING OF TIDAL CHANNELS AND ESTUARIES MORPHODYNAMICS

Alberto Canestrelli
Sergio Fagherazzi
Andrea D'Alpaos

Boulder, October 27th 2011

Tidal channel

- **Mainly affected by tide**
- **Freshwater and river sediment discharge negligible**

Estuary

transition zone between river and ocean

The horizontal scales are much larger than the vertical depth:

vertical acceleration component is relatively **small**.

Hydrostatic pressure distribution on the vertical

If vertical stratification is important → **3D model**

Vertically well mixed → **2D model (vert. averaged)**

TWO DIMENSIONAL SHALLOW WATER EQUATIONS

A SIMPLIFIED HYDRODYNAMIC MODEL

$$\cancel{\frac{\partial u}{\partial t}} + \cancel{\left[u\frac{\partial u}{\partial x} + v\frac{\partial u}{\partial y}\right]} = -g\frac{\partial \eta}{\partial x} - g\frac{u}{\chi^2 D}\sqrt{u^2+v^2} + \cancel{\left(\frac{\partial \mathbf{R}_{xx}}{\partial \mathbf{x}}+\frac{\partial \mathbf{R}_{xy}}{\partial \mathbf{y}}\right)}$$

$$\cancel{\frac{\partial v}{\partial t}} + \cancel{\left[u\frac{\partial v}{\partial x} + v\frac{\partial v}{\partial y}\right]} = -g\frac{\partial \eta}{\partial y} - g\frac{v}{\chi^2 D}\sqrt{u^2+v^2} + \cancel{\left(\frac{\partial \mathbf{R}_{xy}}{\partial \mathbf{x}}+\frac{\partial \mathbf{R}_{yy}}{\partial \mathbf{y}}\right)}$$

$$\frac{\partial}{\partial x}(Du) + \frac{\partial}{\partial y}(Dv) + \frac{\partial D}{\partial t} = 0$$

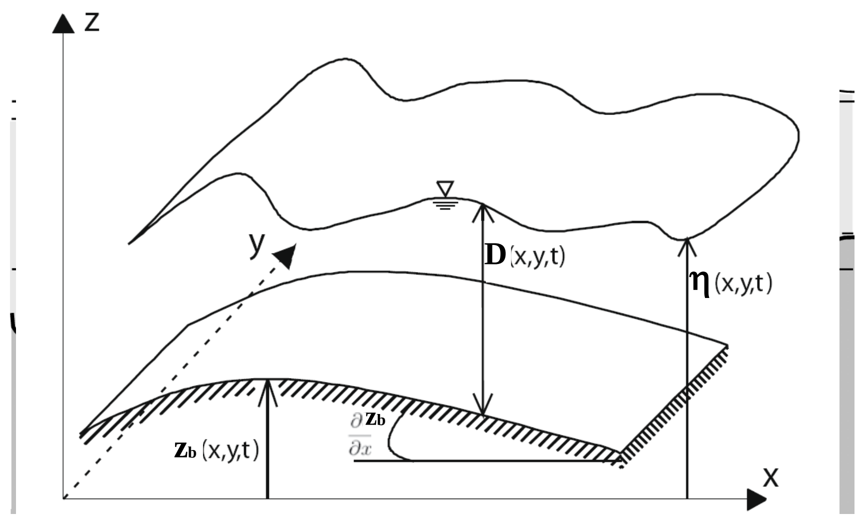

(i) tidal propagation across the intertidal areas flanking the channels is dominated by friction;

(ii) $\eta_1(x,t) << \eta_0(t)-z_0$;

(iii) salt-marsh bottom topography is nearly flat: $z_1(x) << \eta_0(t)-z_0$;

$$\boxed{\nabla^2\eta_1 = \frac{\lambda}{(\eta_0 - z_0)^2}\frac{\partial \eta_0}{\partial t}}$$

Rinaldo et al., *WRR,* 1999a,b

(iv) tidal propagation within the channel network is instantaneous compared to the propagation across the shallow salt marshes or tidal flats;

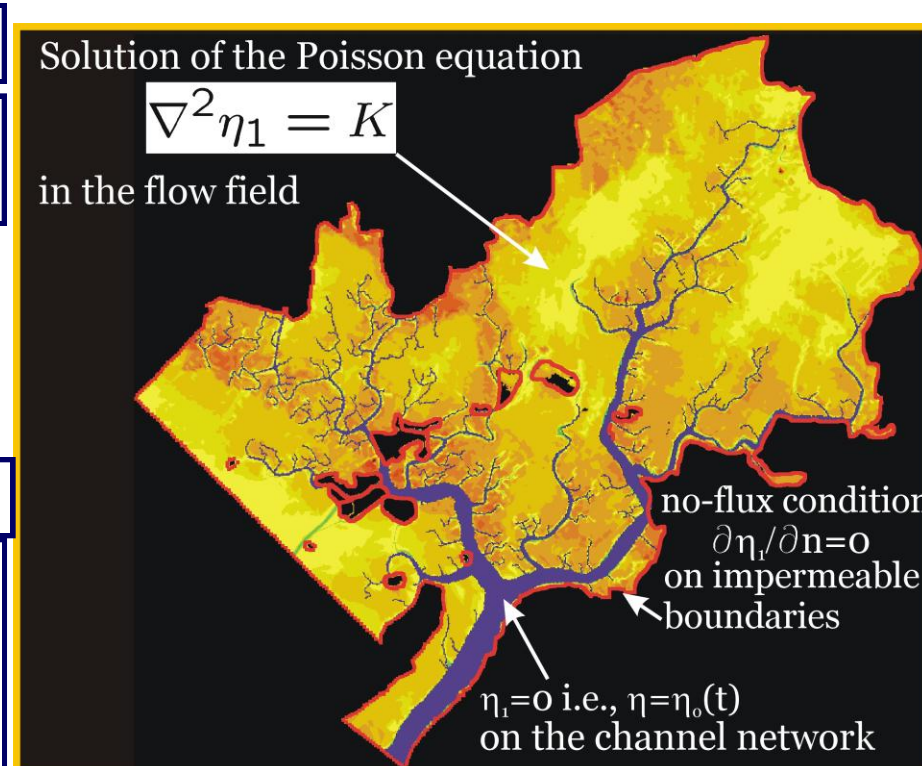

SIMPLIFIED HYDRODYNAMIC MODEL

(Rinaldo et al., *WRR* 1999a,b; Marani et al., *WRR* 2003)

$$\nabla^2 \eta_1 = \frac{\lambda}{(\eta_0 - z_0)^2} \frac{\partial \eta_0}{\partial t}$$

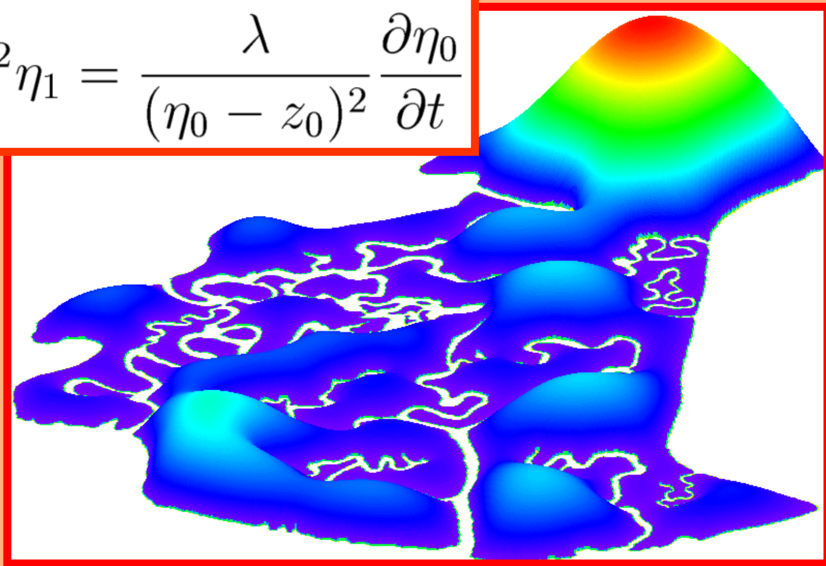

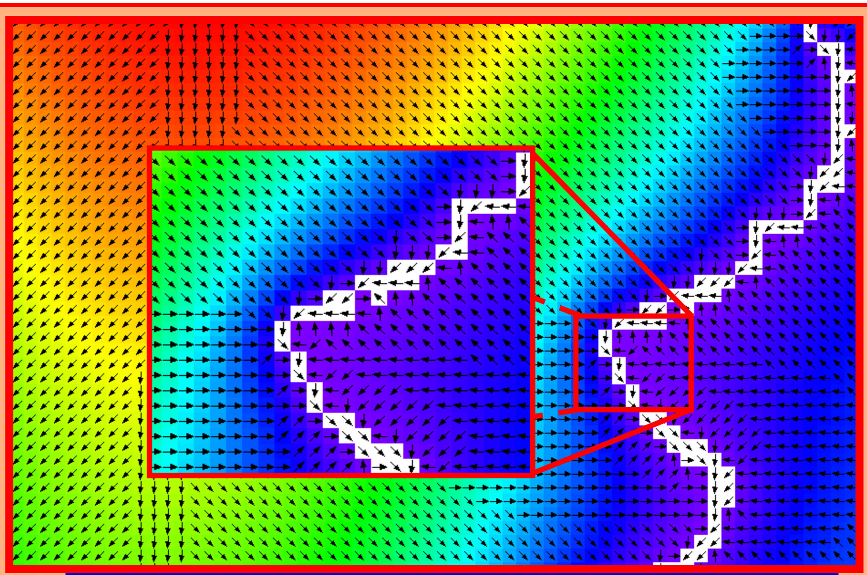

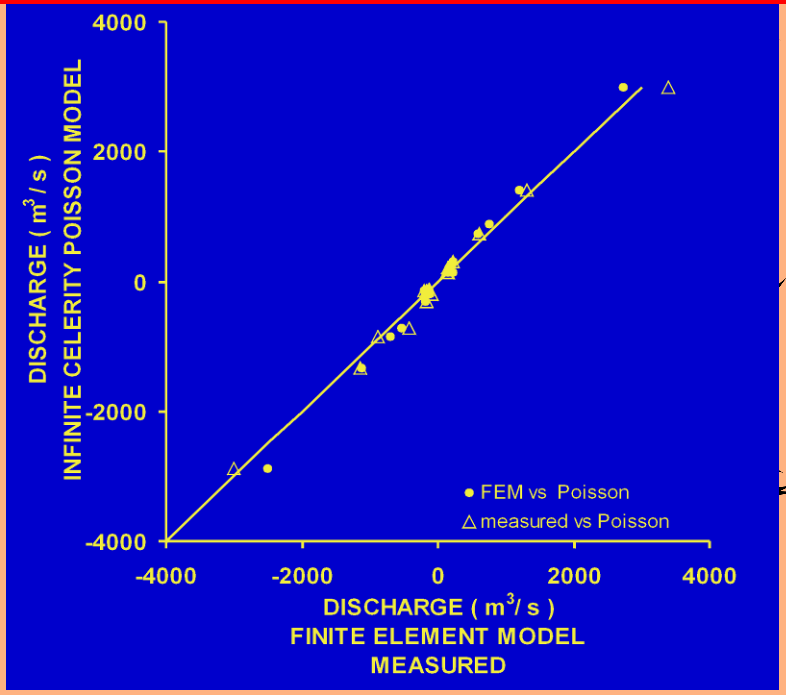

UNCHANNELED PATH LENGTHS or OVERMARSH PATHWAYS

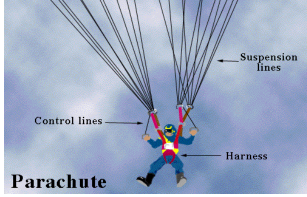

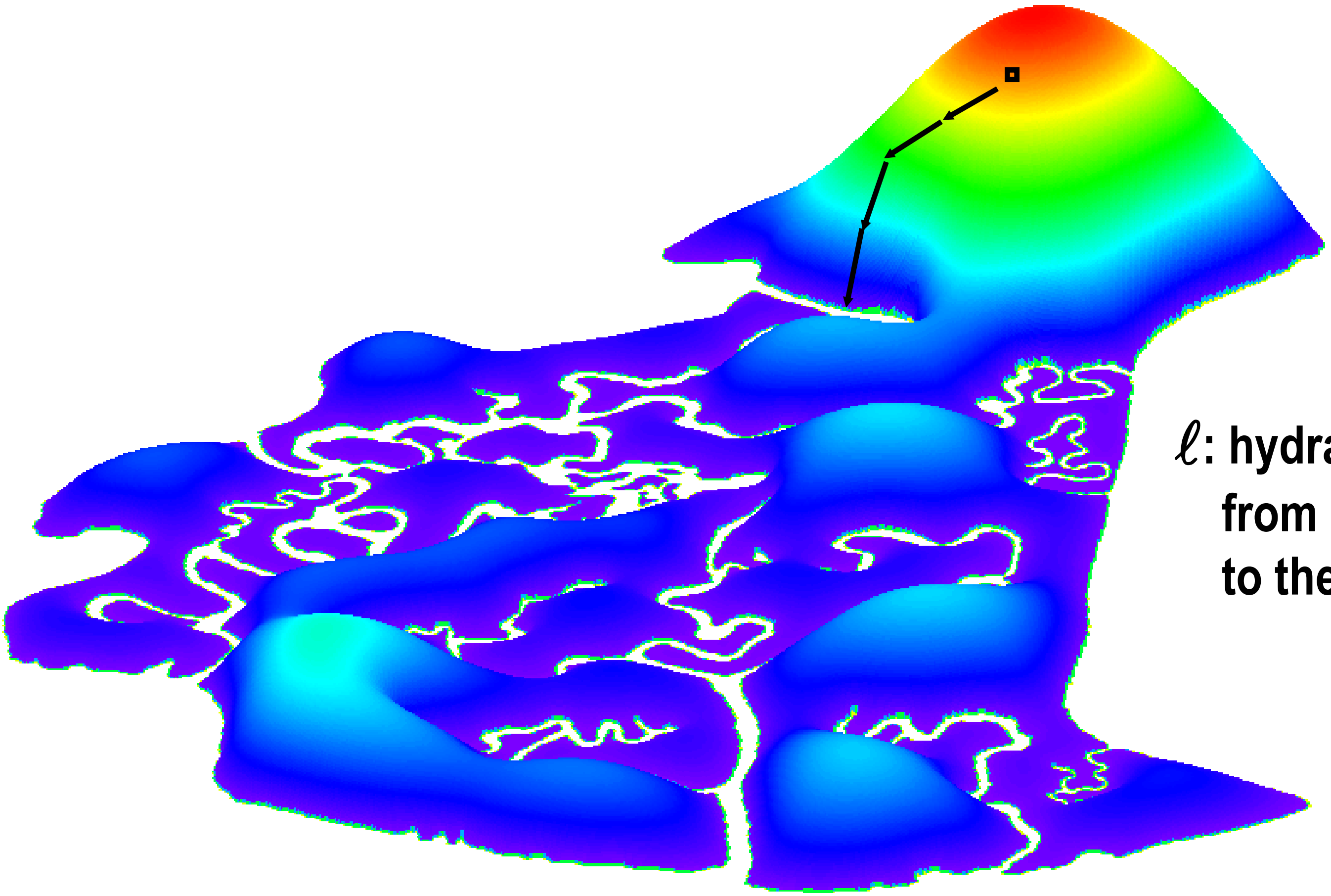

ℓ: hydraulically shorter distance from a point on the salt marsh to the nearest channel

UNCHANNELED PATH LENGTHS

(Marani et al., *WRR* 2003)

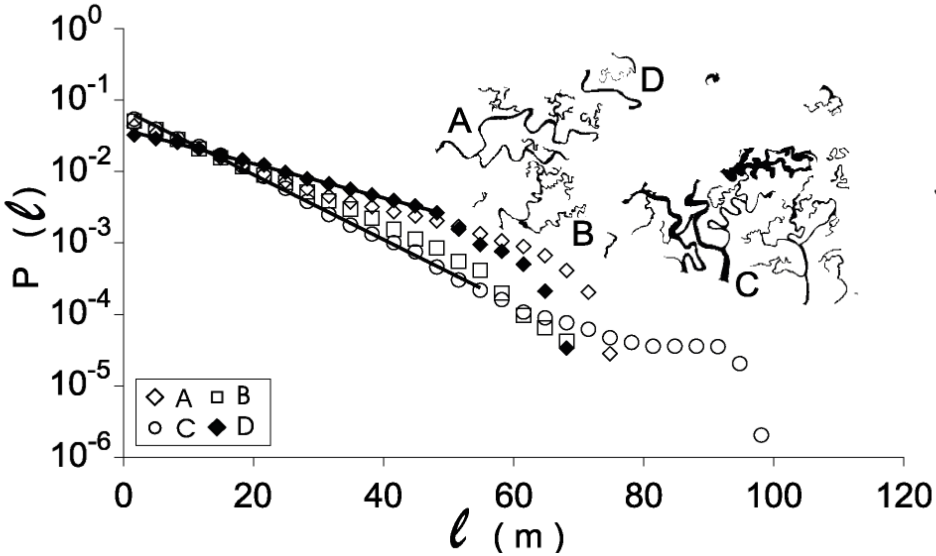

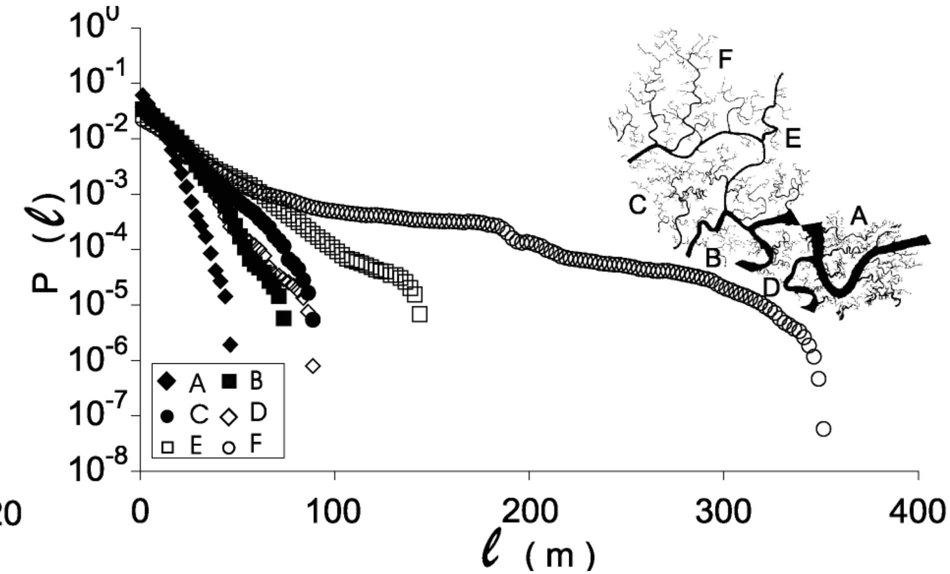

The probability distributions of unchanneled lengths are typically characterized by the tendency to develop **exponential decays**

Absence of scale-free network features

The mean unchanneled drainage length tends to fluctuate considerably even in adjacent sites

Space-dependent processes influence network development

CHANNEL NETWORK ONTOGENY MODEL (INITIATION & EARLY DEVELOPMENT)

Timescale of initial network incision << Timescale of
- channel meandering
- marsh-platform growth
- changes in external forcing (e.g., RSLR)

Decouple the initial network incision from slower processes

- Headward channel growth driven by exceedences of a critical shear stress
- Instantaneous adaptation of the channel cross-sections to the local tidal prism

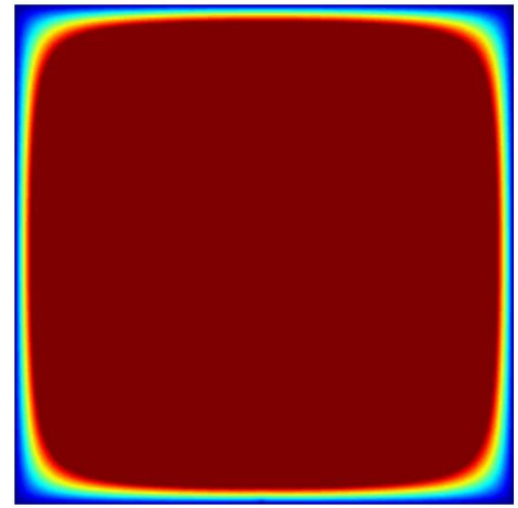

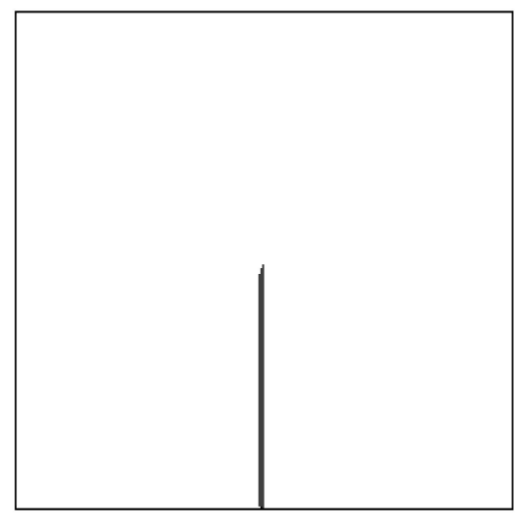

- Landscape-forming events are due to spring peak discharges
- Comparison to observed morphologies performed on the basis of the pdf of unchanneled flow lengths

LOCAL VALUE OF THE BOTTOM SHEAR STRESS

$$\tau(\mathbf{x}) = \rho g \left[\eta_0 + \eta_1(\mathbf{x}) - z(\mathbf{x})\right] \nabla \eta_1(\mathbf{x})$$

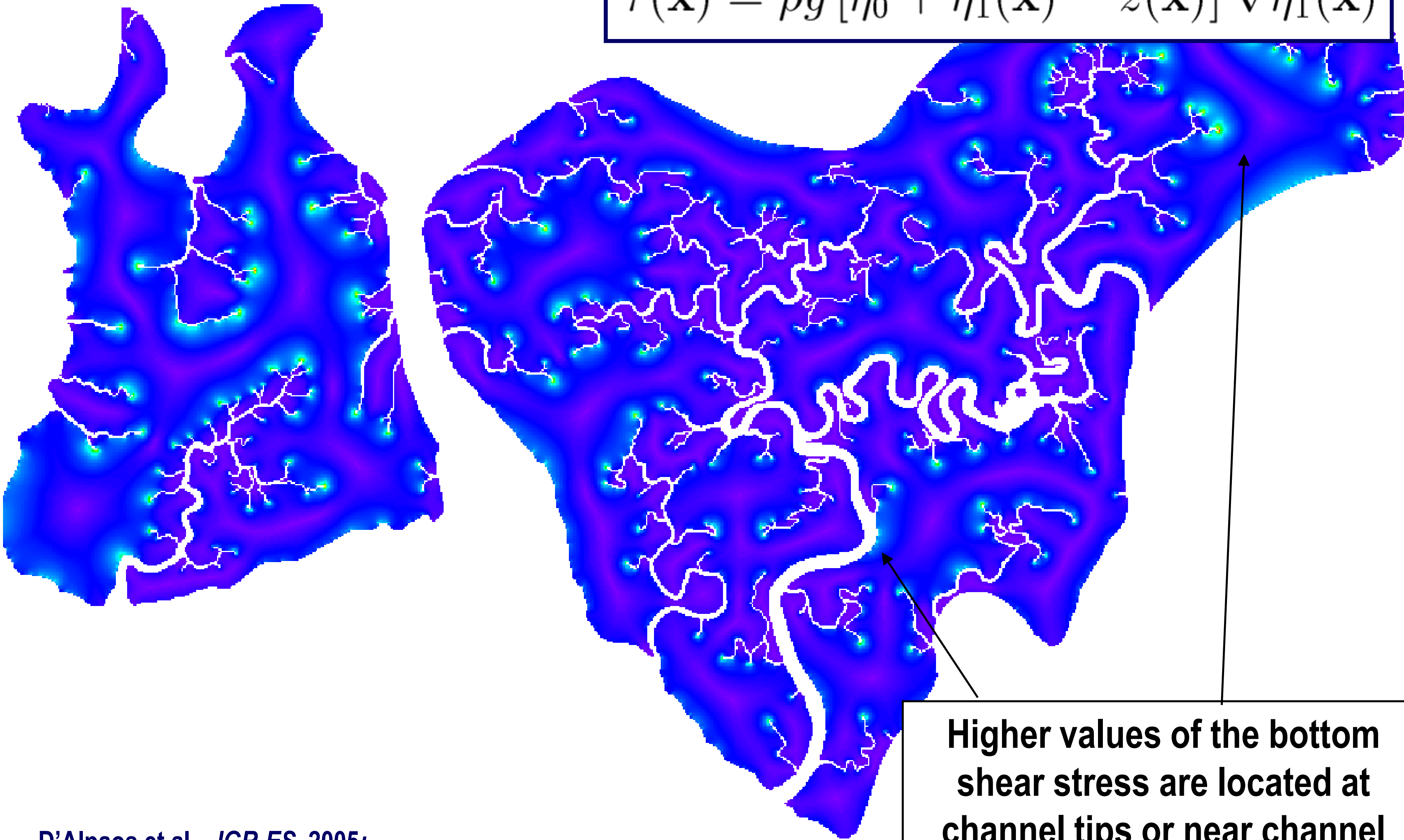

Higher values of the bottom shear stress are located at channel tips or near channel bends

D'Alpaos et al., *JGR-ES*, 2005;
Feola et al., *WRR*, 2005

HEADWARD GROWTH CHARACTER of NETWORK DEVELOPMENT

Hughes et al,. *GRL* 2009

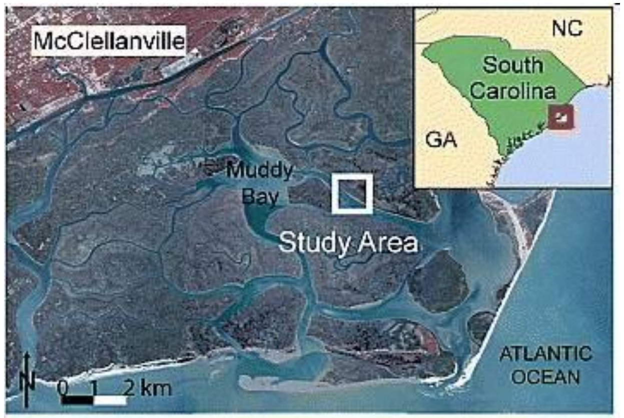

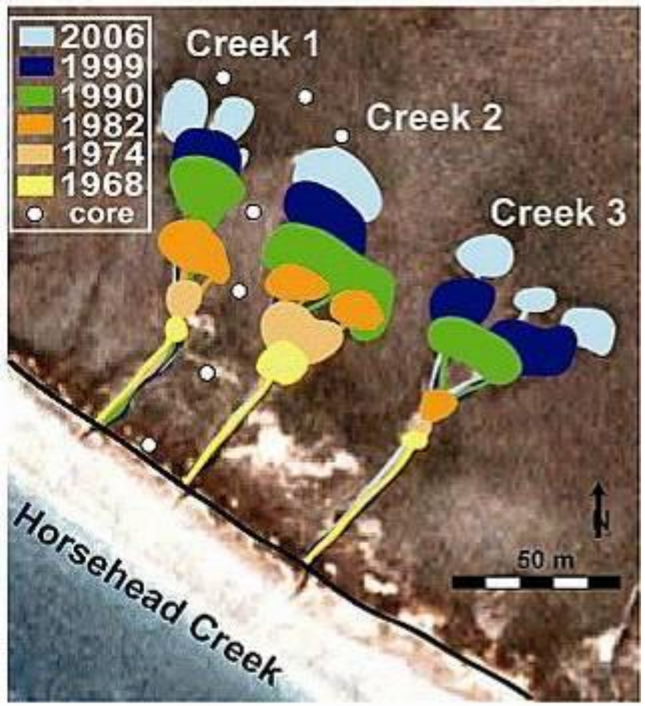

(e.g. Steers, 1960; Pestrong, 1965; French and Stoddart, 1992; Collins et al. 1987; Wallace et al. 2005; D'Alpaos et al., 2007)

O'BRIEN-JARRETT-MARCHI LAW

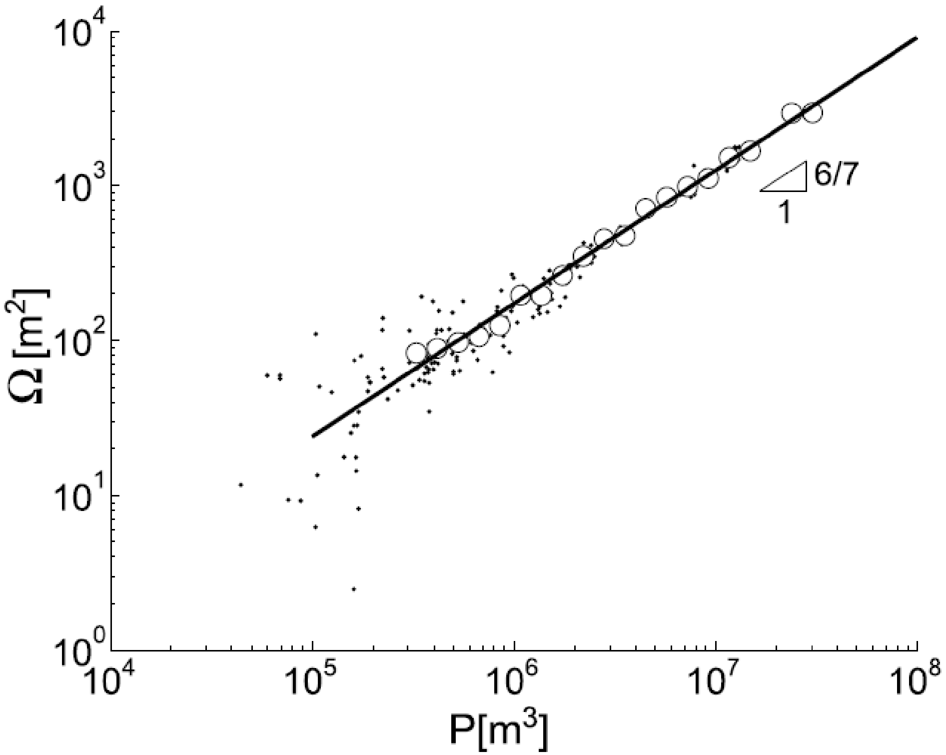

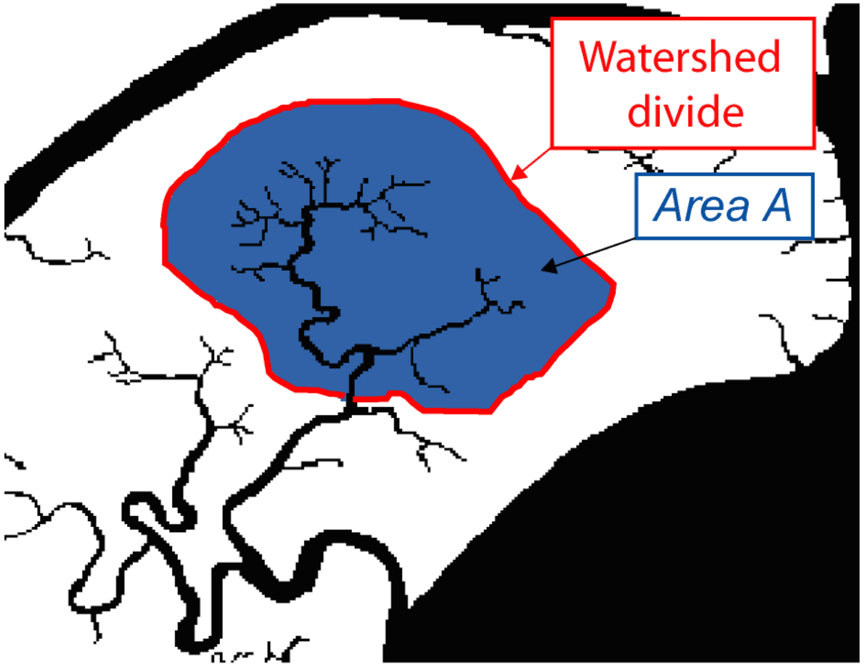

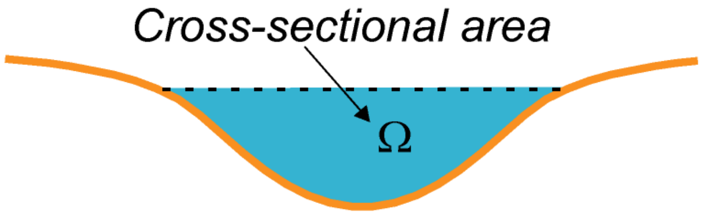

$$\Omega \propto Q_{\max}$$

Myrick & Leopold, 1963; Rinaldo et al., 1999

$$\Omega = k\ P^{\alpha}$$

O'Brien, 1969; Jarrett, 1976; Marchi 1990; D'Alpaos et al., *Rendiconti Lincei*, 2009; D'Alpaos et al., *JGR* 2010

MODELLING THE SPONTANEOUS GROWTH OF A TIDAL CREEK NETWORK WITHIN A NEWLY CONSTRUCTED MARSH IN THE VENICE LAGOON

A **network** of **volunteer creeks** established themselves away from an artificially constructed main channel (quite rapidly *O(1)* year).

The **rapid formation** of such a tidal-creek system provided a **unique opportunity** to **test** the reliability of the **model** of tidal network initiation and development

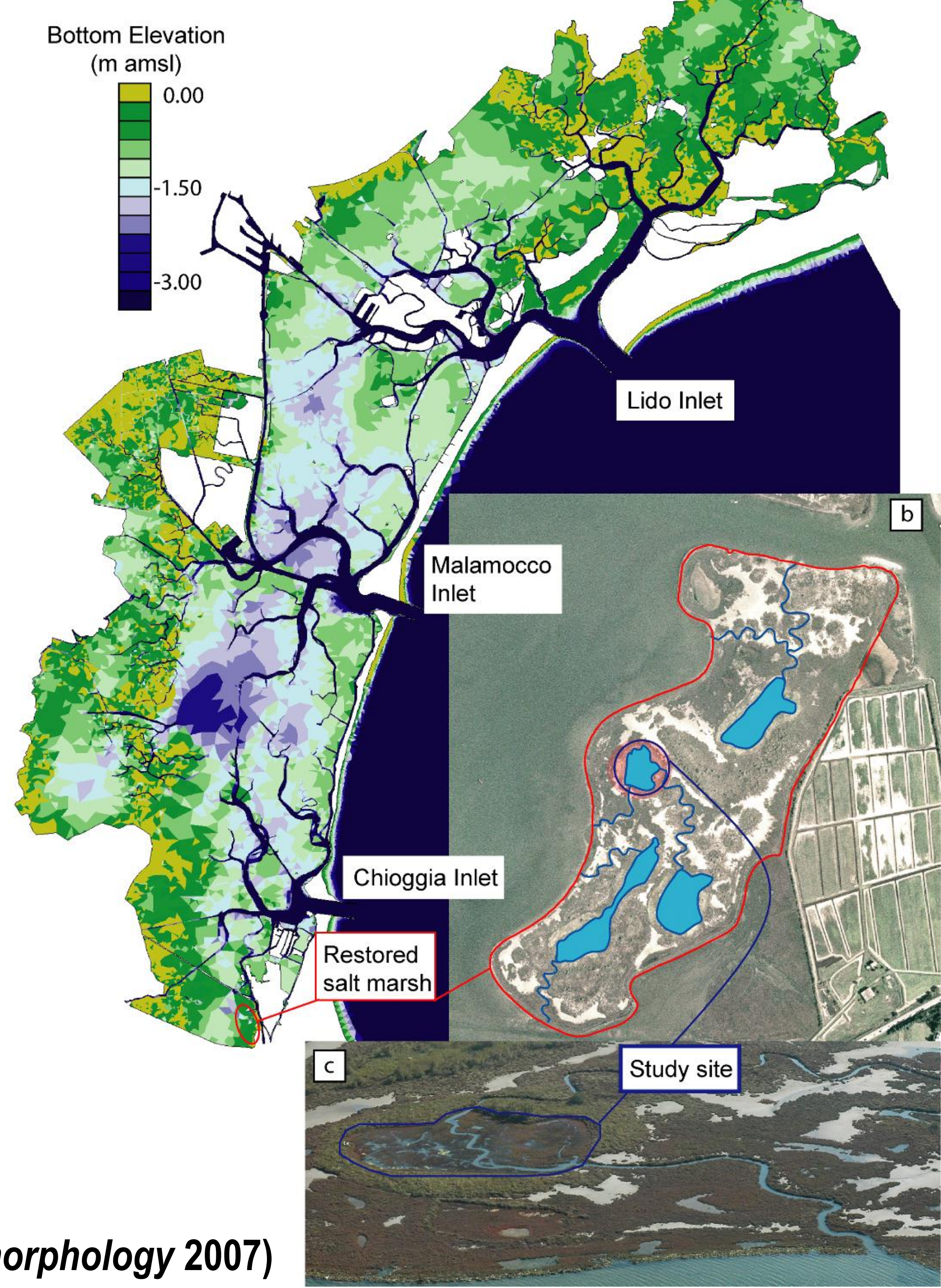

(D'Alpaos et al., *Geomorphology* 2007)

OBSERVED EVOLUTION OF THE CREEK NETWORK

artificially reconstructed channel

(a) Aerial photograph of the study site (2000)

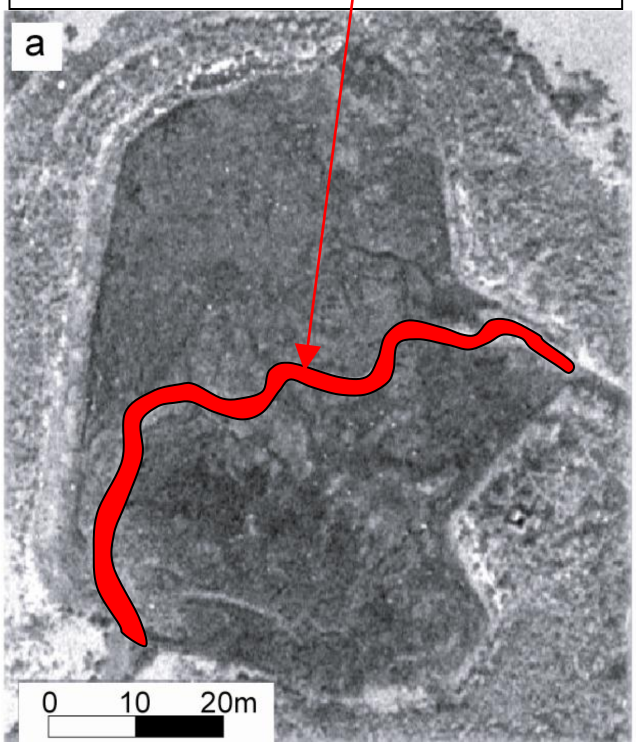

(b) Aerial photograph of the study site (2002)

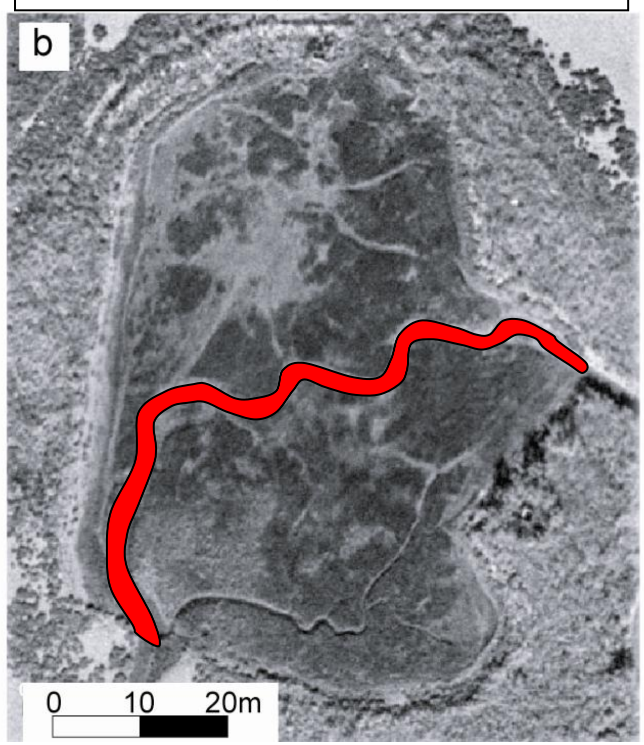

(c) Network extraction (based on 2002 image)

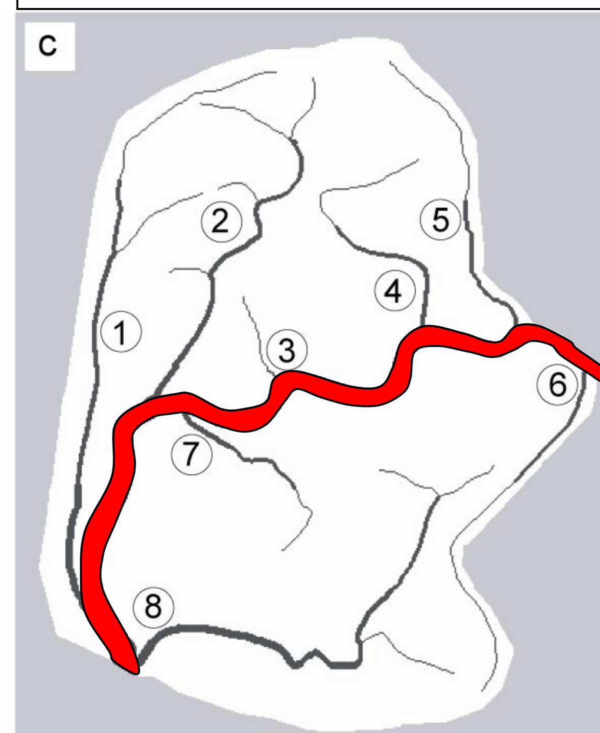

MODELING vs OBSERVATIONS

Synthetic creek networks

$\tau_c = 0.15$ Pa; $T = 0.01$ m | $\tau_c = 0.15$ Pa; $T = 0.05$ m | $\tau_c = 0.15$ Pa; $T = 0.1$ m

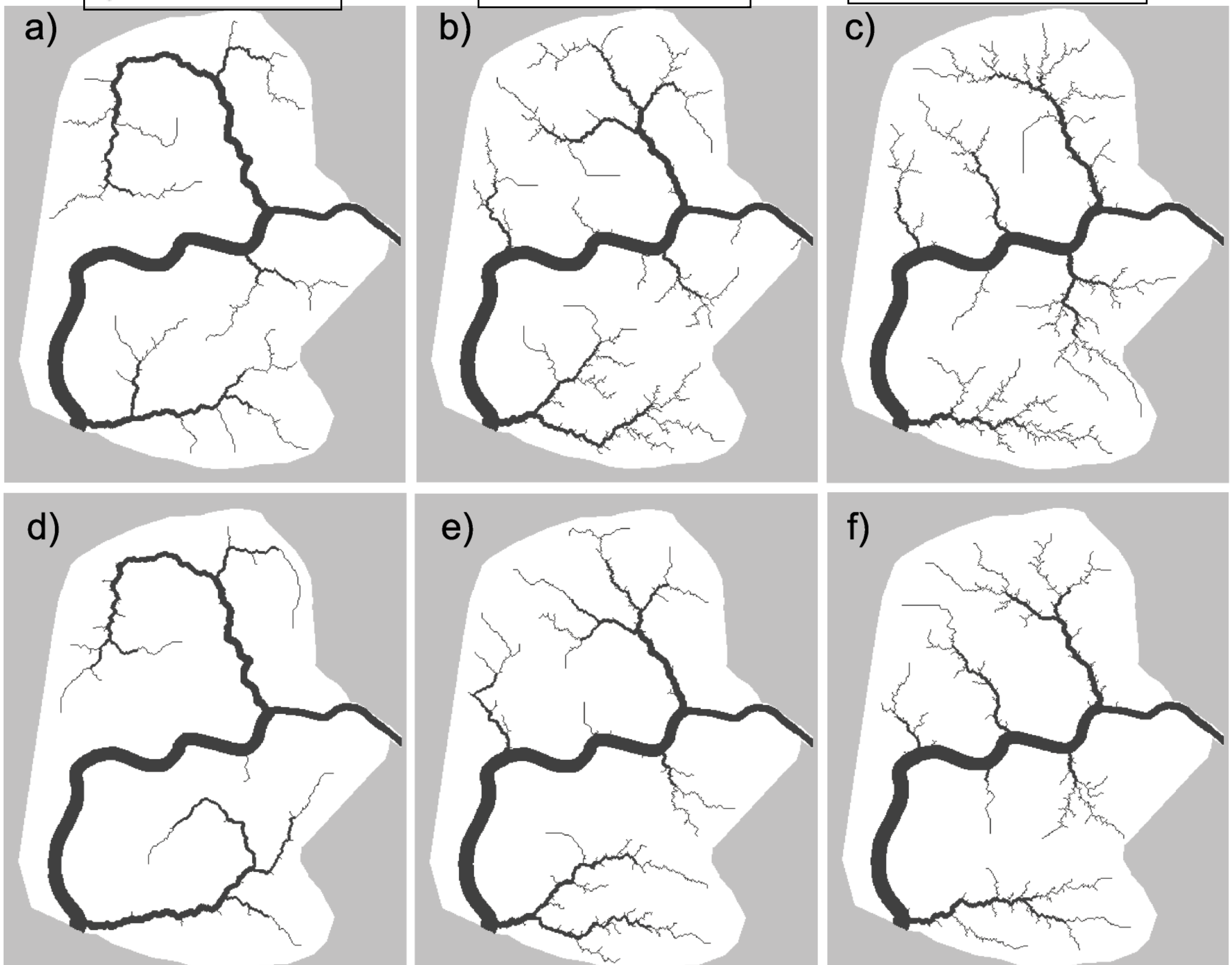

$\tau_c = 0.25$ Pa; $\tau_c = 0.01$ m | $\tau_c = 0.25$ Pa; $T = 0.05$ m | $\tau_c = 0.25$ Pa; $T = 0.1$ m

Spontaneous creek networks

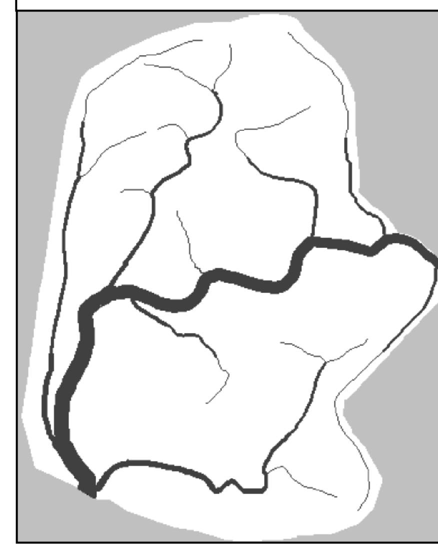

MODELING vs OBSERVATIONS

Objective comparison to observed morphologies based on the pdf of unchanneled lengths

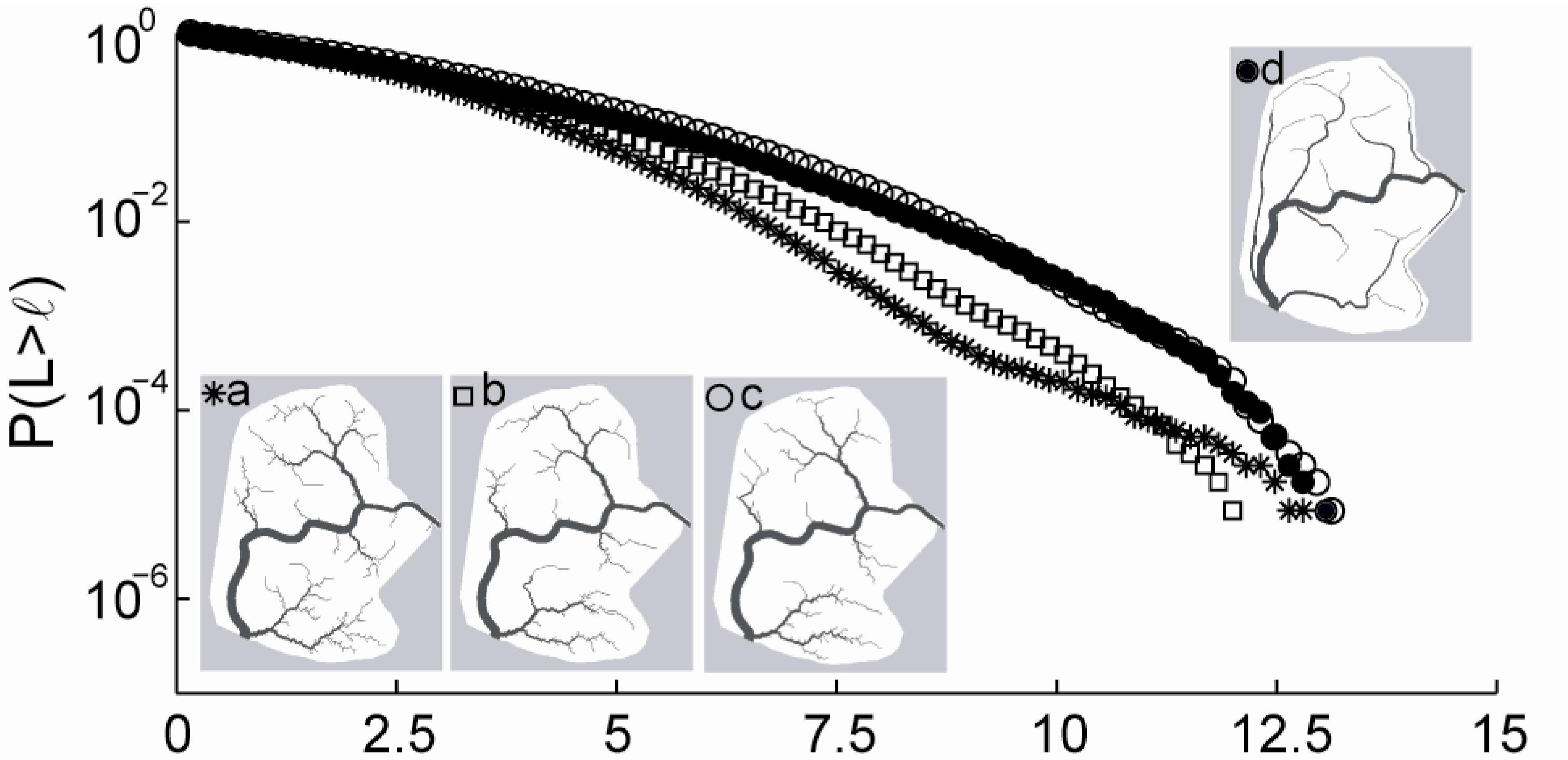

Rather than a pointwise reproduction of network features, the model predicts realizations whose statistical properties are similar to those of actual networks.

This allows us to indirectly access the validity of model assumptions.

Laboratory observations of the morphodynamic evolution of tidal channels (Tambroni et al 2005)

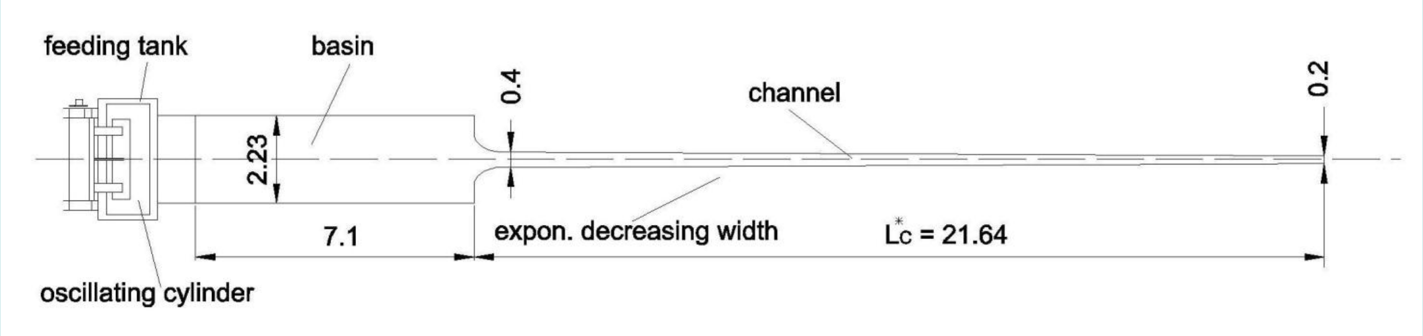

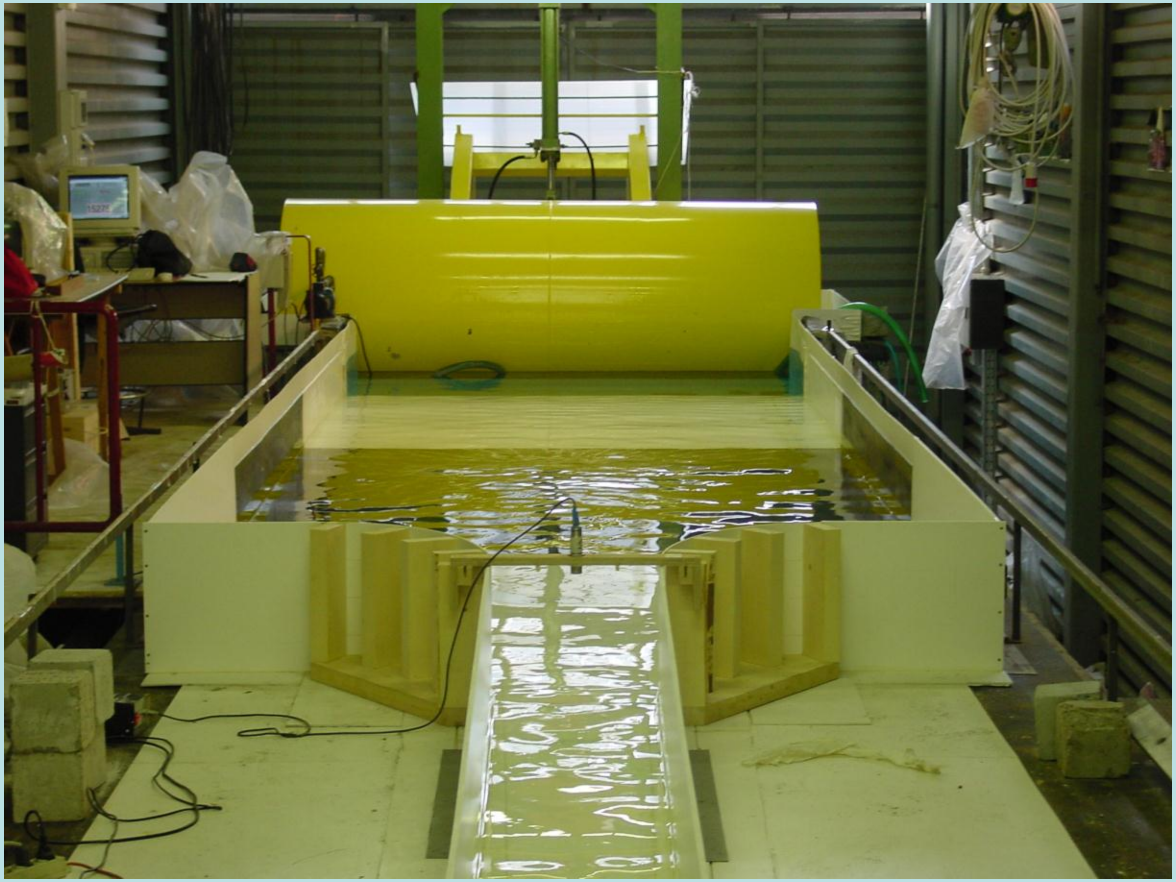

Mean water level:

$D_0 = 0.09$ m

Sinusoidal oscillation in the basin:

$a_0 = 0.032$ m

$T = 120$ s

Choesionless bed material:

d_s=0.3 mm

ρ=1480 kg/m

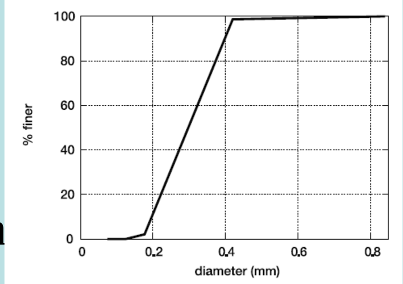

Mathematical-numerical model

Hydrodynamic → Shallow water equations

$$\frac{\partial q_x}{\partial t}+\frac{\partial}{\partial x}\left(\frac{q_x^2}{Y}\right)+\frac{\partial}{\partial y}\left(\frac{q_x q_y}{Y}\right)-\left(\frac{\partial R_{xx}}{\partial x}+\frac{\partial R_{xy}}{\partial y}\right)+gY\frac{\partial h}{\partial x}+\frac{\tau_{bx}}{\rho}=0$$

$$\frac{\partial q_y}{\partial t}+\frac{\partial}{\partial x}\left(\frac{q_x q_y}{Y}\right)+\frac{\partial}{\partial y}\left(\frac{q_y^2}{Y}\right)-\left(\frac{\partial R_{xy}}{\partial x}+\frac{\partial R_{yy}}{\partial y}\right)+gY\frac{\partial h}{\partial y}+\frac{\tau_{by}}{\rho}=0$$

$$\eta\frac{\partial h}{\partial t}+\frac{\partial q_x}{\partial x}+\frac{\partial q_y}{\partial y}=0$$

Y = effective water depth= $\frac{\text{Volume}}{\text{Area}}$

η = local fraction of wetted domain

Assuming that bottom elevations are distributed according to a Gaussian probability density function we obtain [Defina 2000]:

$$\eta=\frac{1}{2}\left(1+erf\left(\frac{2D}{a_r}\right)\right)$$

$$\frac{Y}{a_r}=\left\{\eta(D/a_r)+\frac{1}{4\sqrt{\pi}}\exp\left[-4(D/a_r)^2\right]\right\}$$

With:

$$\vec{\tau}_b=g\left(\frac{|q|}{k_s^2 H^{10/3}}\right)\vec{q}\rho Y$$

$$H/a_r\approx Y/a_r+0.27\sqrt{Y/a_r}\cdot e^{-2Y/a_r}$$

Where H is an equivalent water depth [Defina 2000]:

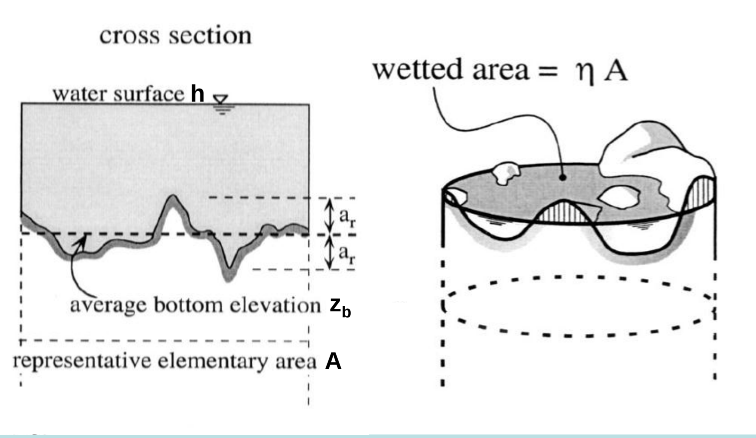

a_r=amplitude of ground irregularity = $2\sigma_b$

D = average water depth =$h-z_b$

z_b= average bottom elevation

Morphodynamic

Exner equation

$$(1-n)\frac{\partial z_b}{\partial t}+\nabla\cdot\vec{q}_b+(r_E-r_D)=0$$

Diffusion-advection equation for suspended-load:

$$\frac{\partial(YC)}{\partial t}+\frac{\partial}{\partial x}(q_xC)+\frac{\partial}{\partial y}(q_yC)-\frac{\partial}{\partial x}\left(YD_x\frac{\partial C}{\partial x}\right)-\frac{\partial}{\partial y}\left(YD_y\frac{\partial C}{\partial x}\right)=r_E-r_D$$

Where:

$\mathbf{q}_b=\mathbf{q}_b(\cos\alpha,\mathrm{sen}\alpha)$ = bed-load rate for unit width

C = depth averaged concentration of suspended-load

D_x , D_y = eddy diffusivity along x and y

n = porosity

settling velocity [Van Rijn 1984]

r_E-r_D = entrainment and deposition = $w_s(C_{eq}-C_a)$

concentration at y=a [Parker et al. 1987]

equilibrium concentration [Van Rijn 1984]

The intensity of bed load rate q_b is expressed by [Struiskma 1985]:

$$q_b=q_{bo}(1-\chi c_F\frac{\partial z_b}{\partial s})$$

$\mathbf{q_{b0}}$ $\longrightarrow$ Van Rjin (1993)

s = streamwise direction

$c_F=k_s^2Y^{1/3}/g$ = friction factor

χ = 0.03 according to Struiksma and Crosato, 1989.

Hydrodynamics

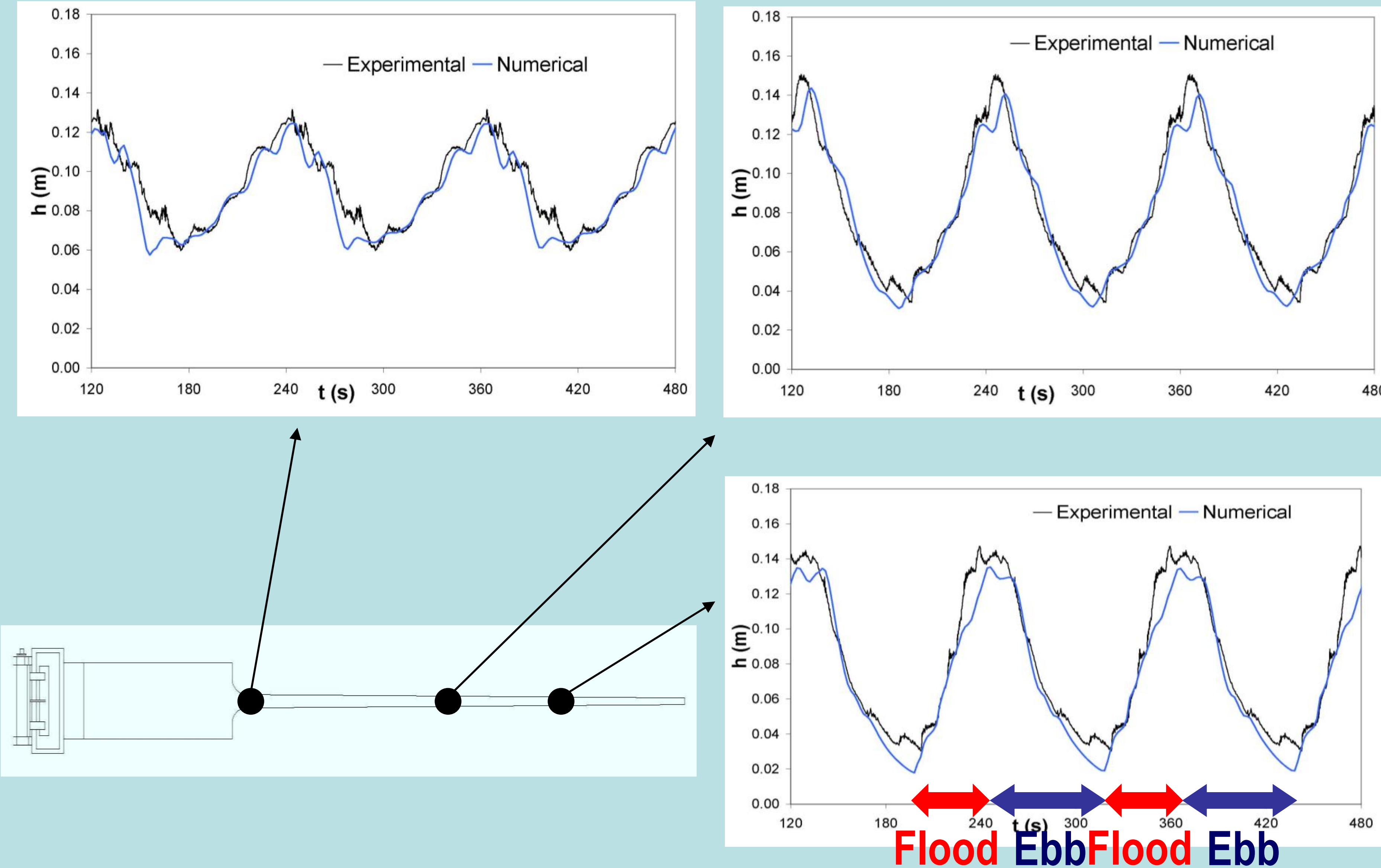

Maximum ebb

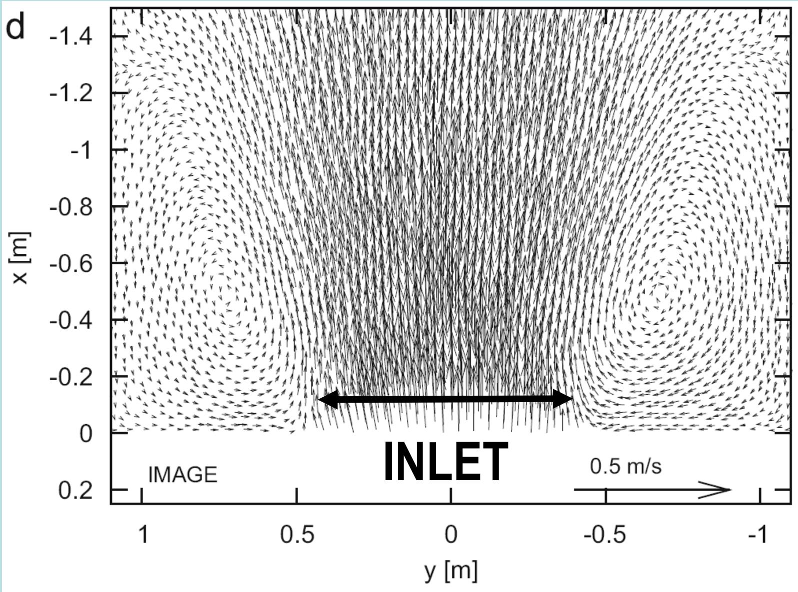

End of ebb

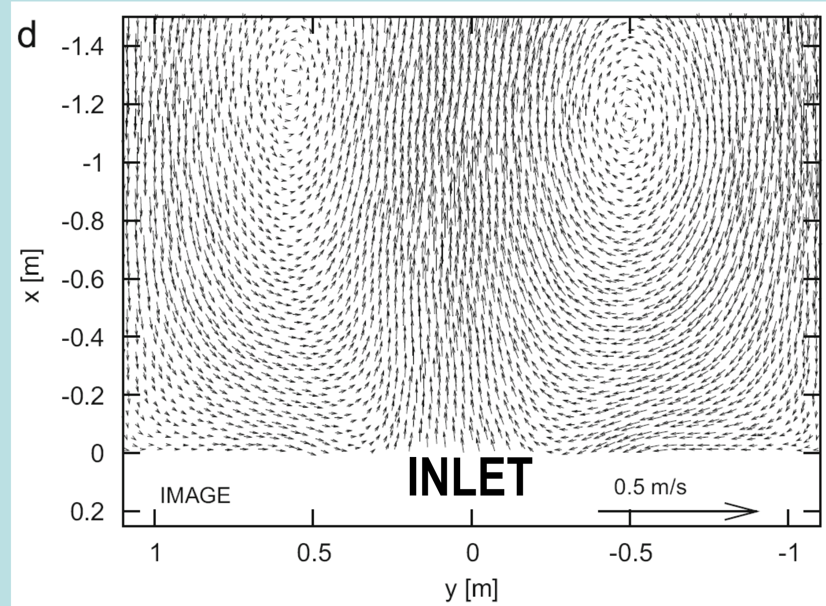

Beginning of flood

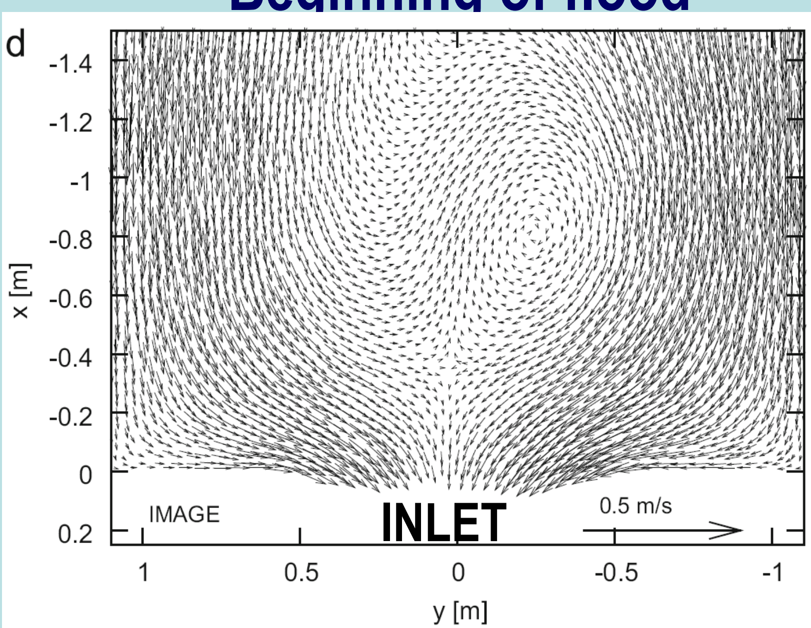

Maximum flood

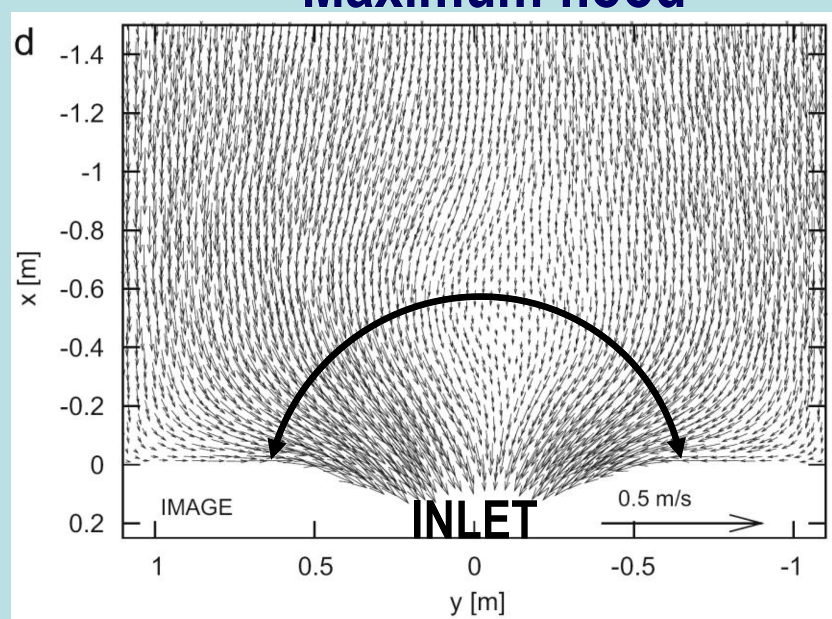

Morphodynamic evolution of the channel

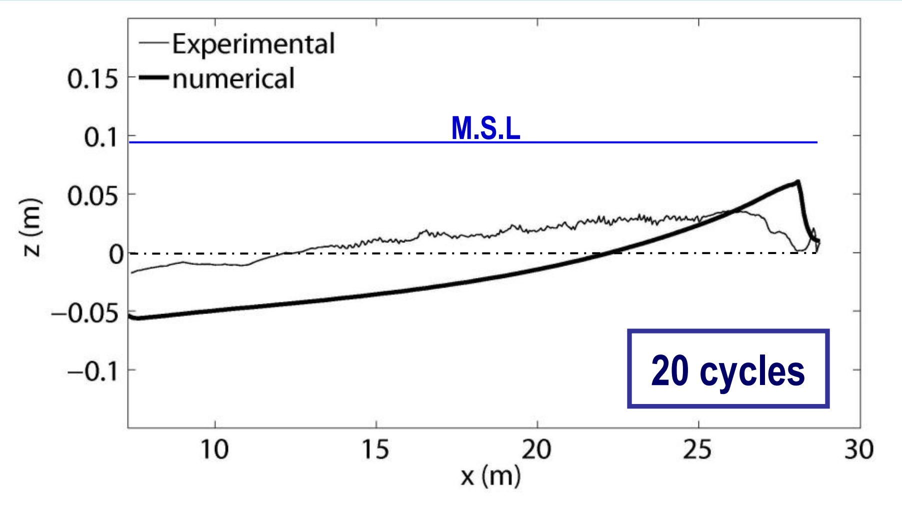

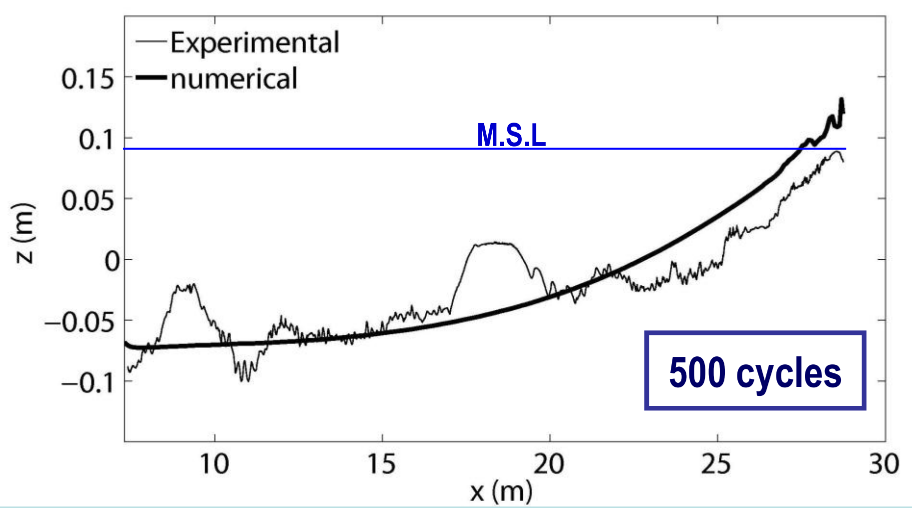

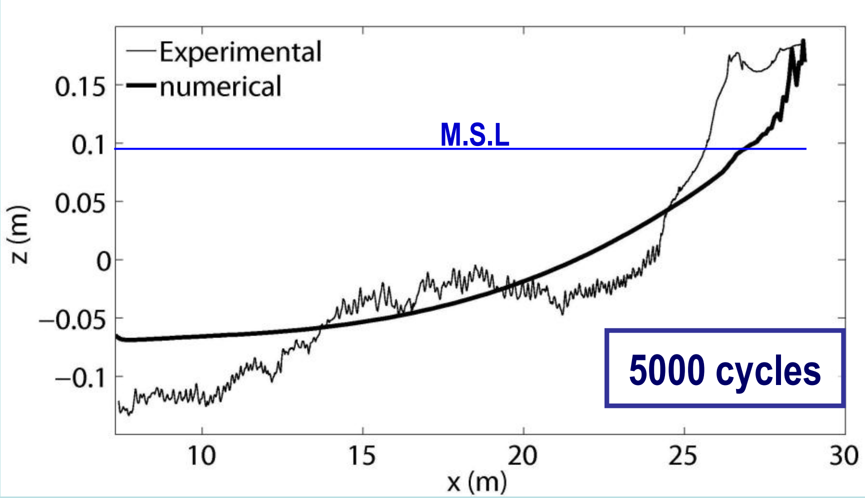

Equilibrium configuration

Tambroni, Ferrarin and Canestrelli, CSR, 2009

EVOLUTION OF A TIDAL CHANNEL FLANKED BY TIDAL FLATS (Canestrelli et al. 2009)

Water level: $h=a \sin(2\pi t/T)$, T=12 h , a = 0.5 m
$C=C_{eq}$ during the flood phase; during the ebb phase it is calculated by the numerical model.

No flux conditions for both water and solid phase

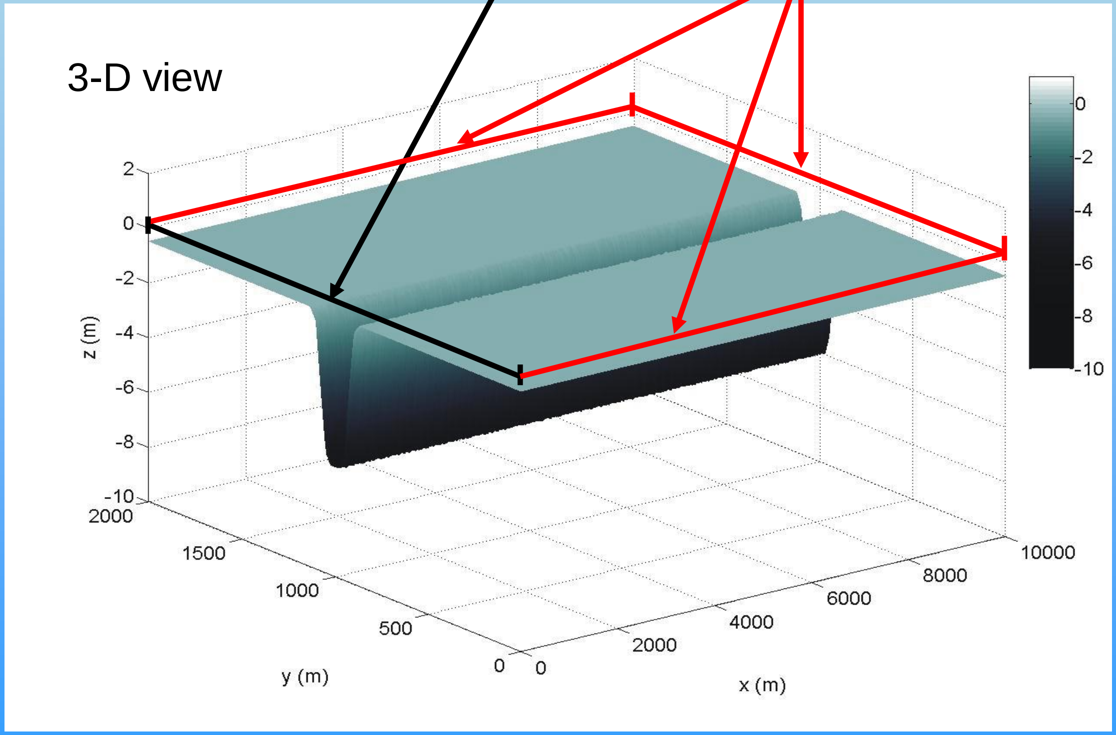

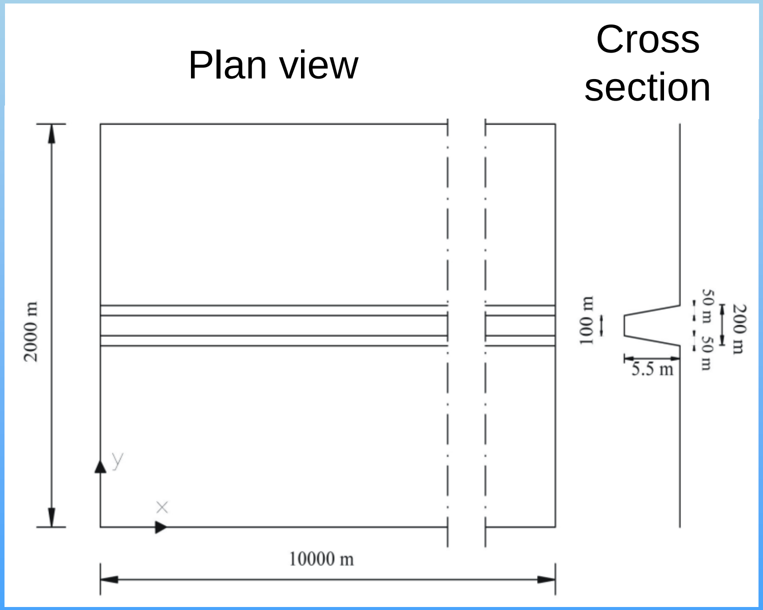

We neglect:
-presence of vegetation
-resuspension of sediment by wind wave motion

Parameters:

K_s=30 $m^{1/3}s^{-1}$; d_s=0.064 mm (uniform sand) a_r=0.3 m

Cell resolution varies gradually from 30 m into the channel to 80 m at the boundary of tidal flats.

Longitudinal profile of tidal channel

Deposition

Sediment front propagating landward

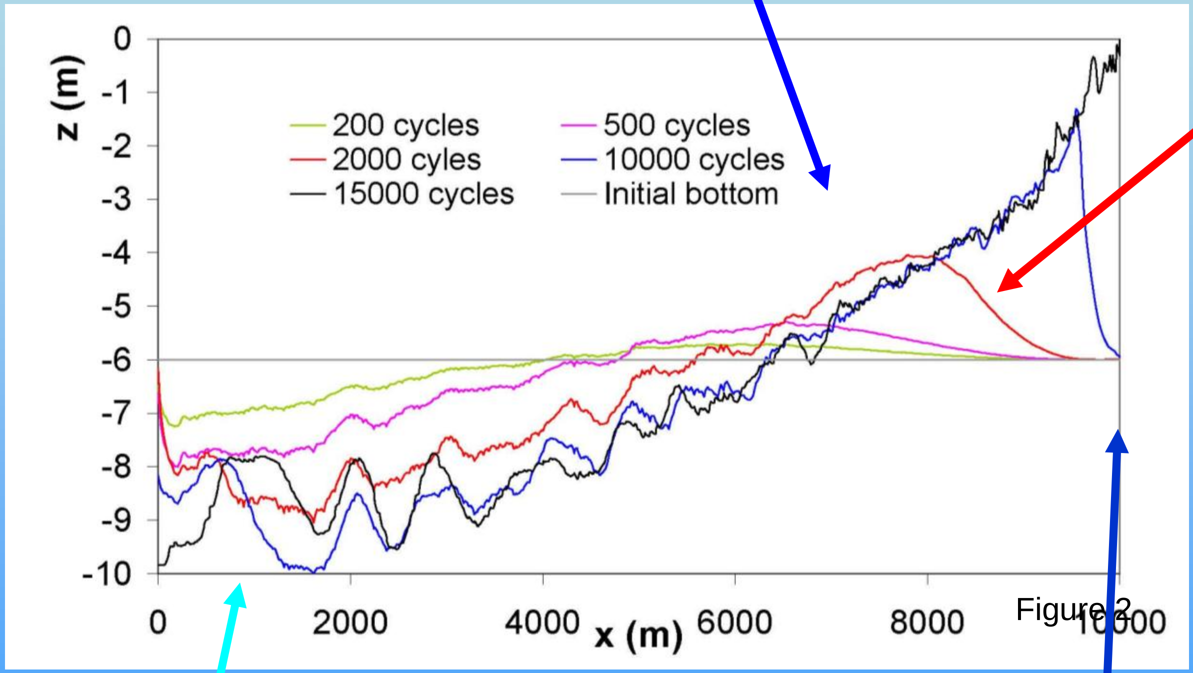

Scour near the inlet

Bed evolution is slower and slower as equilibrium is approached

Velocity along the tidal channel

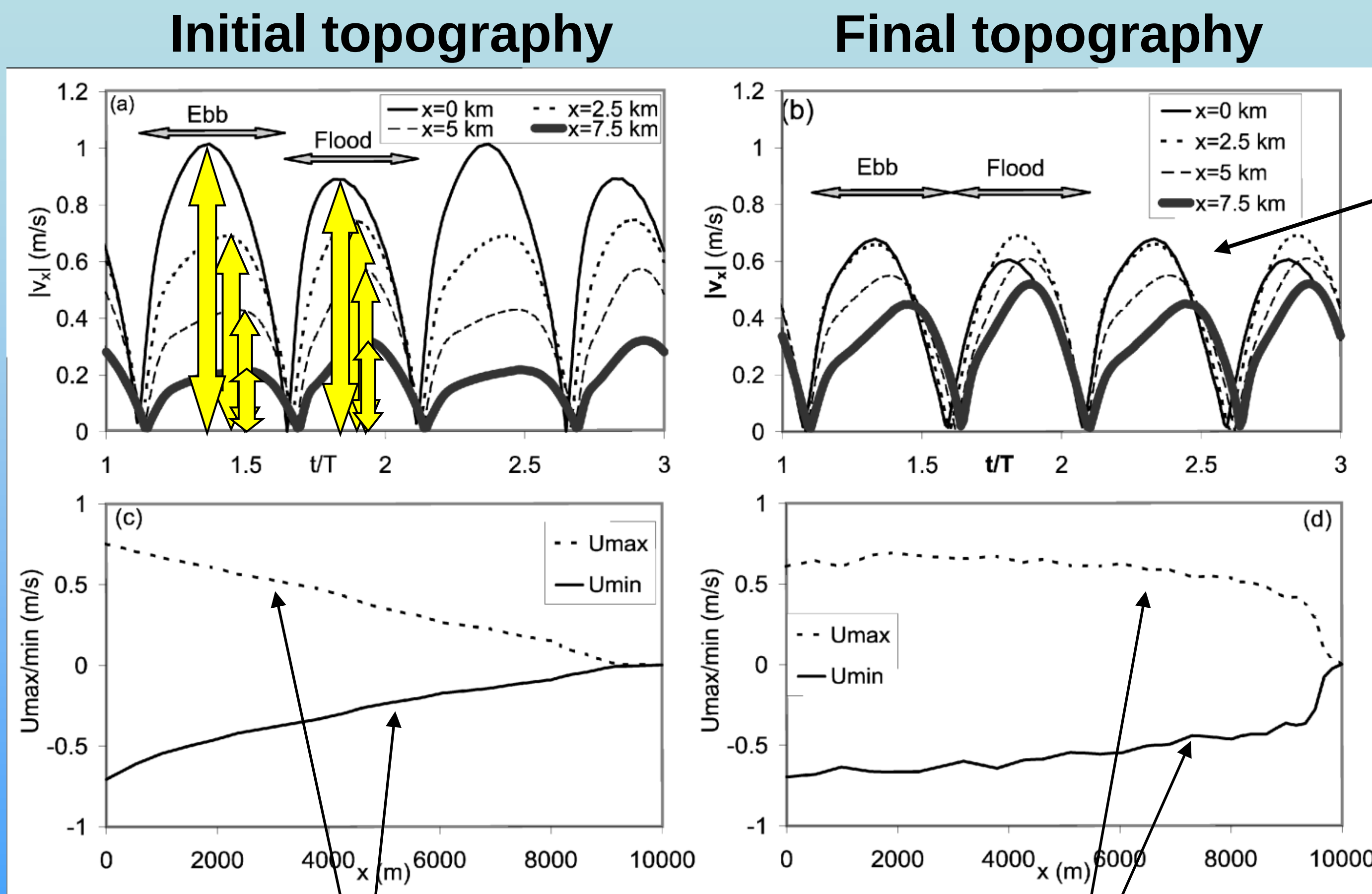

Reduction of ebb/flood asymmetry

Almost linear decrease along x

Tendency toward a spatially constant velocity peaks

Shear stress, sediment discharge and water level

Initial topography **Final topography**

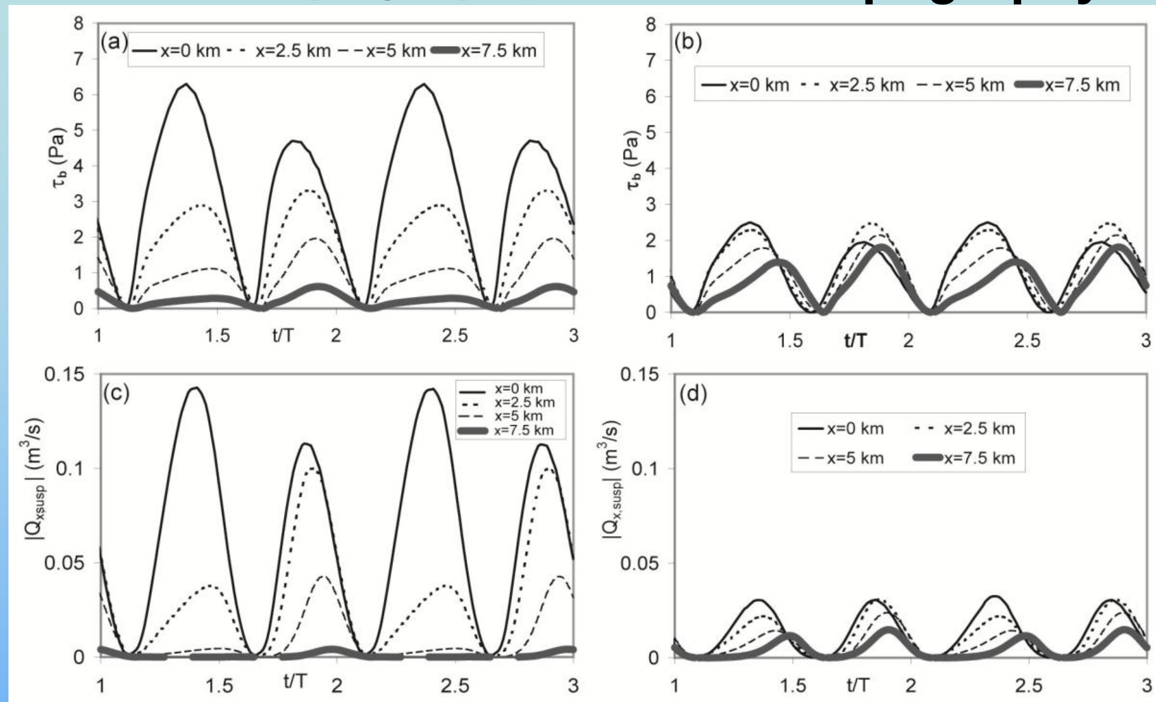

Net (tidally averaged) sediment discharge (m^3/s)

	x=0 km	*x*=2.5 km	*x*=5 km	*x*=7.5 km
Qsa (initial bottom)	-0.0111	0.0114	0.0069	0.0007
Qsa (final bottom)	-0.0007	0.0011	0.0014	0.0006

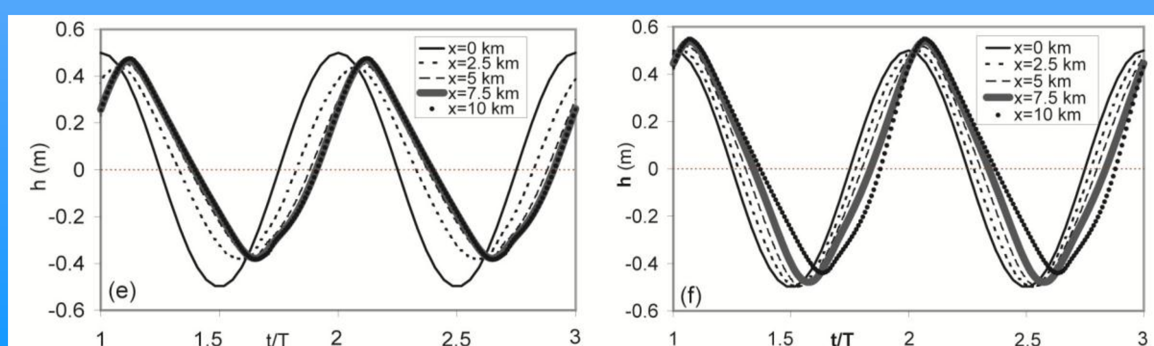

Evolution of the tidal flats

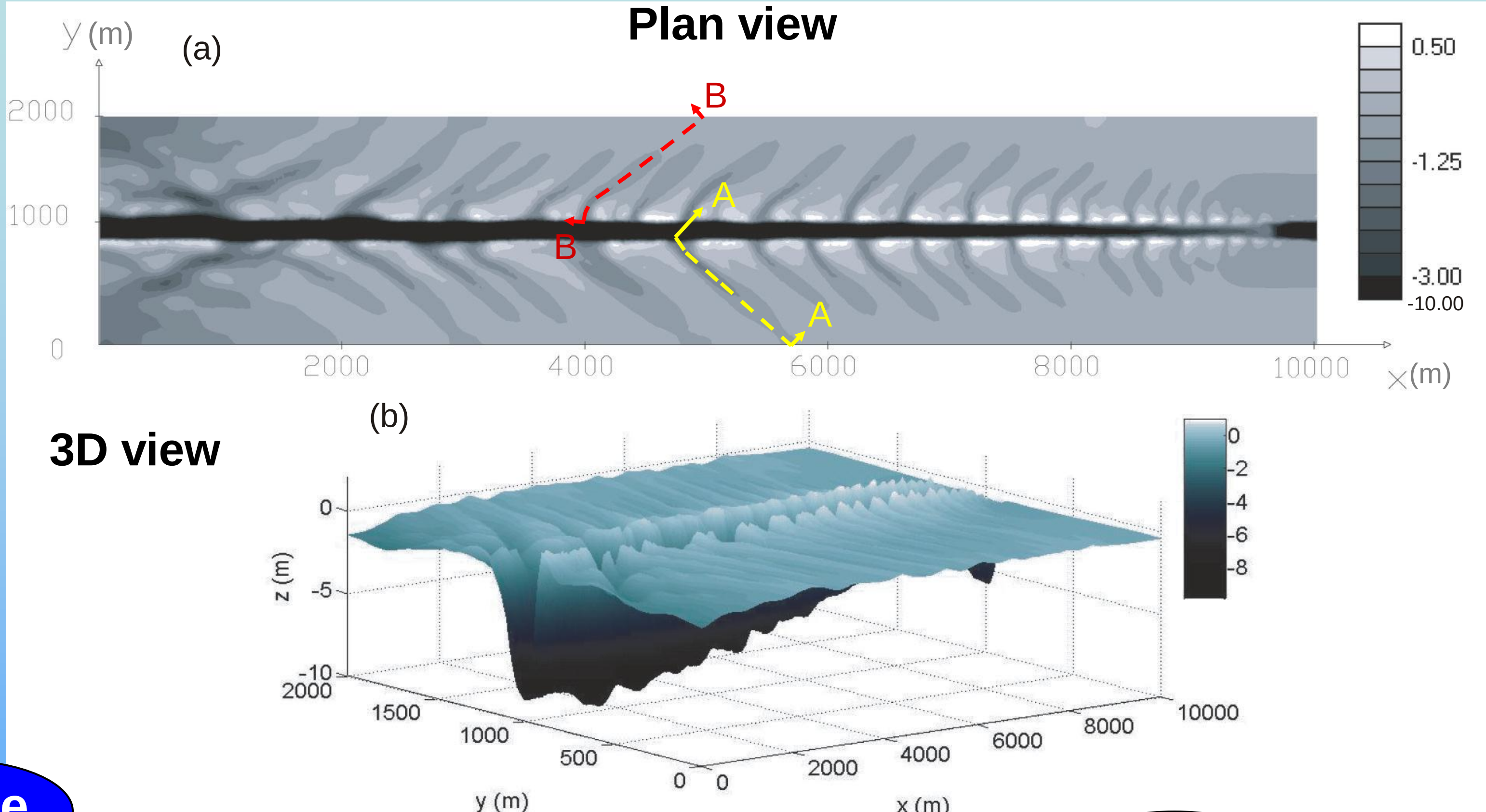

Levee

Section A-A:

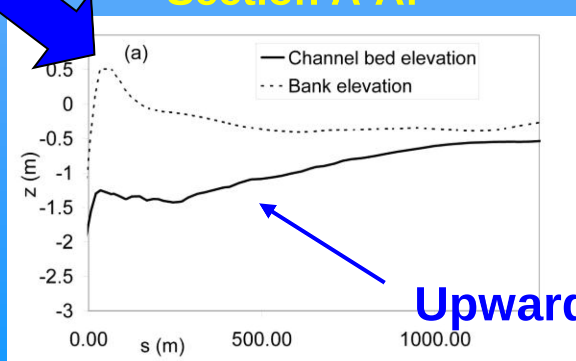

S

Levee

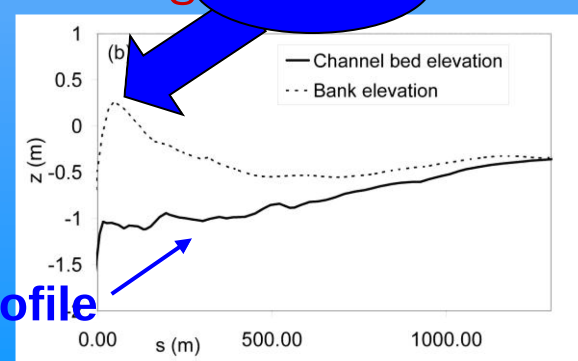

Upward concave profile

Main channel funneling

$$B = B_0 \exp\left(-\frac{x}{L_b}\right)$$

Exponential trend: ***L_b=9668 m***

It favors the increase of tidal amplitude

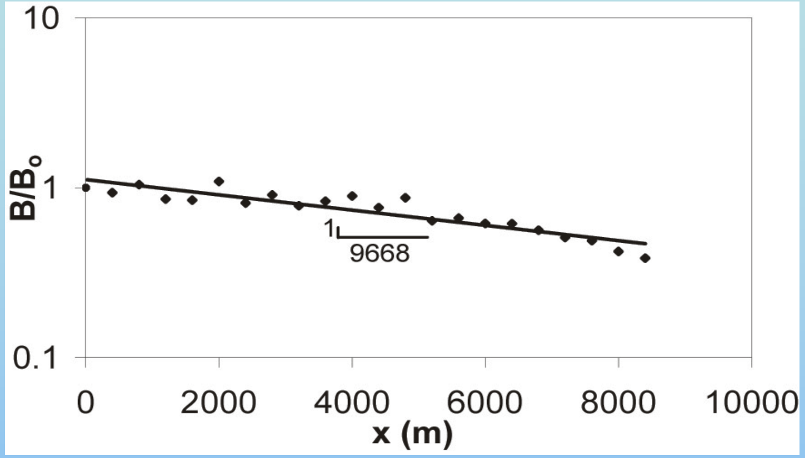

Linear relationship between the cross sectional area at creek inlet and creek watershed area [Rinaldo et al., 1999]

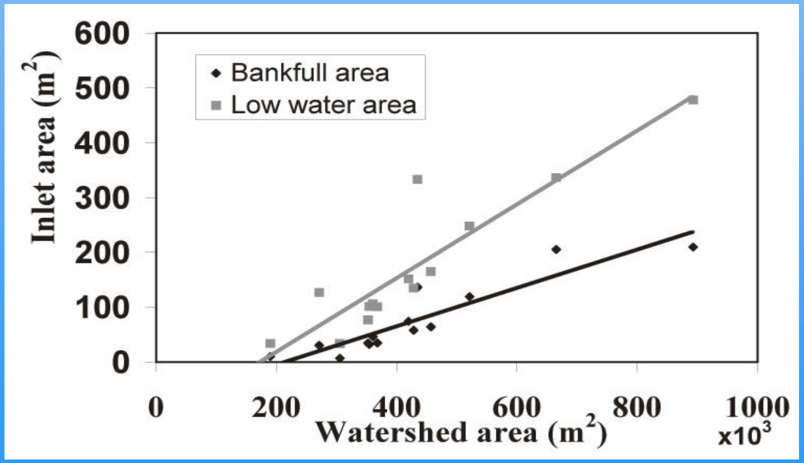

THE FLY RIVER ESTUARY

- The Fly river and his tributaries are tropical rivers characterized by a remarkably small variation in flow discharge.

mean annual freshwater discharge = $\boxed{\textbf{6000 - 6500 m}^3\textbf{/s}}$ $\pm$ 25% (seas. var.)

(Lower Fly River) (Wolanski et al. 1997)

- The Fly River is the 17th largest river in the world in terms of sediment discharge

Qs: $\boxed{\text{85 million tonnes a}^{-1}}$ (Galloway 1975)

- The basin is characterized by a rapid rate of erosion: **3-4 mm/a** (Pickup, 1984)

⇨ high rainfall in the highlands: $\boxed{\textbf{> 10 m a}^{-1}}$ (Harris et al., 1993)

⇨ easily weathered volcanic, sedimentary and weakly metamorphosed bedrock.

- Modest catchment area: $\boxed{\textbf{79,000 km}^2}$

FLY RIVER DELTA

TIDAL REGIME

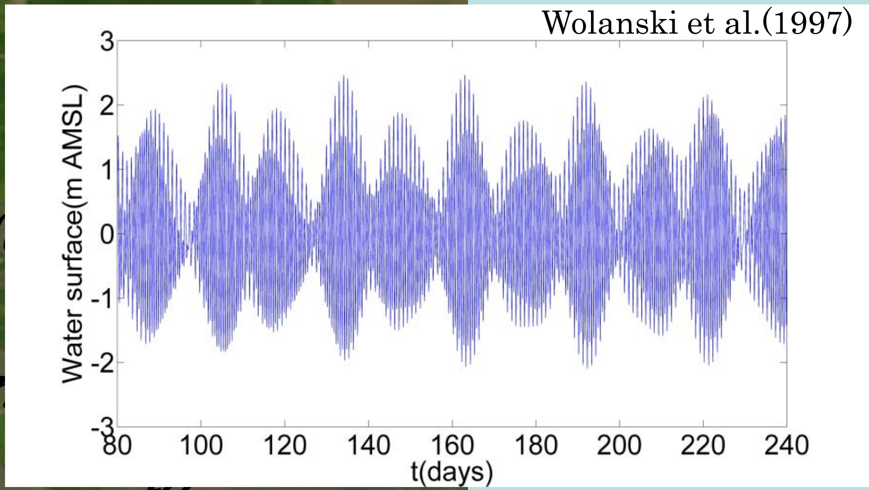

Neap tide

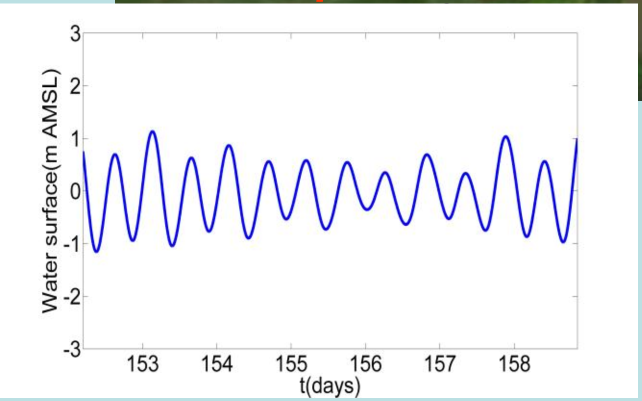

Spring tide

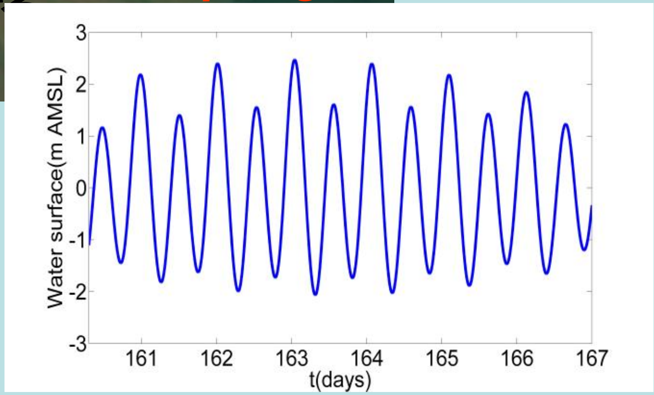

Tidal range 1-1.5m

Tidal range 4-5m

- Because of the low gradient the tidal influence is felt up to 300-400 km inland.

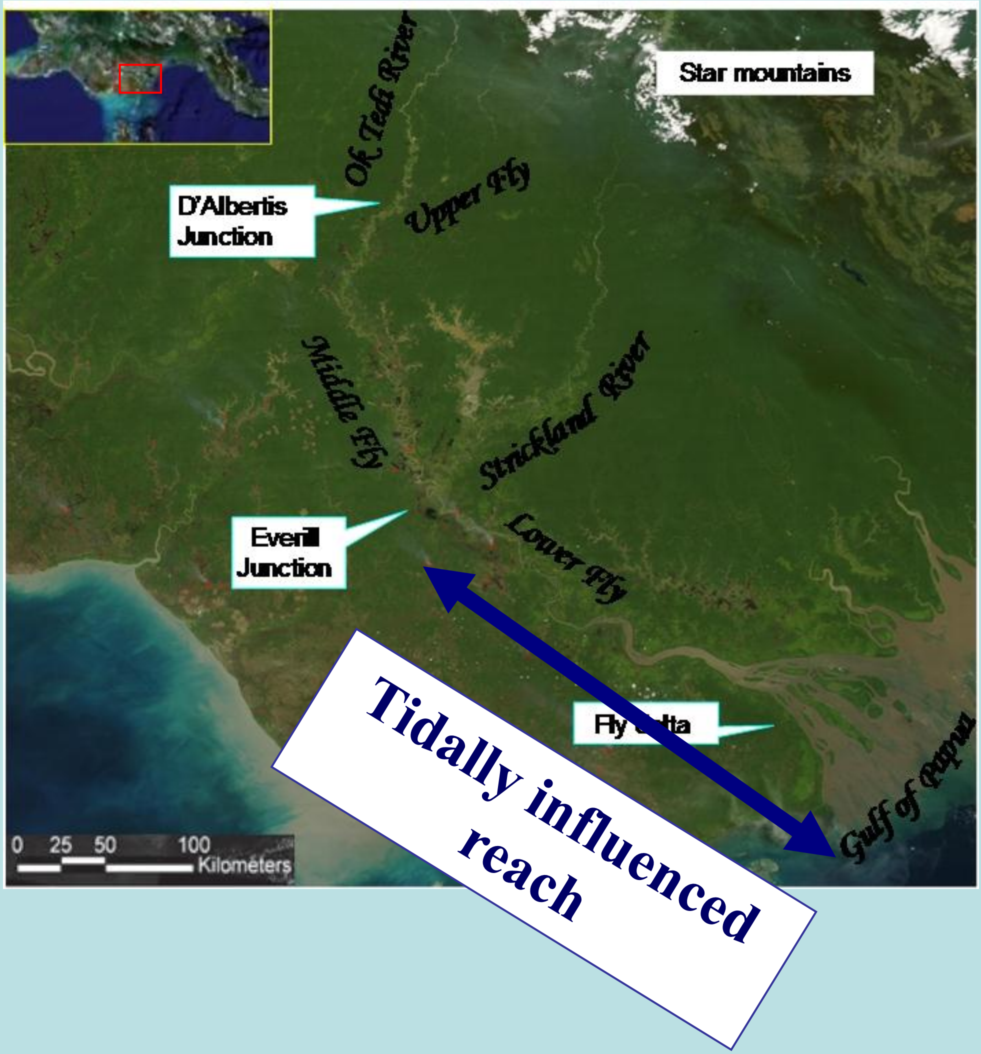

- The delta front displays 6-8 m/y of progradation of the deltaic sediments across the shelf (Harris et al. 1993) ➤ net seaward sediment transport

Model assumptions

- The model does not consider the wind waves propagation and generation.

  The wave energy in the distributary channels is minimal (Thorn and Wright, 1983)

  - distributary-mouth bars block all but short-period waves
  - scarcity of beaches

- The model do not consider the effect of stratification and density-driven baroclinic currents.

well-mixed conditions

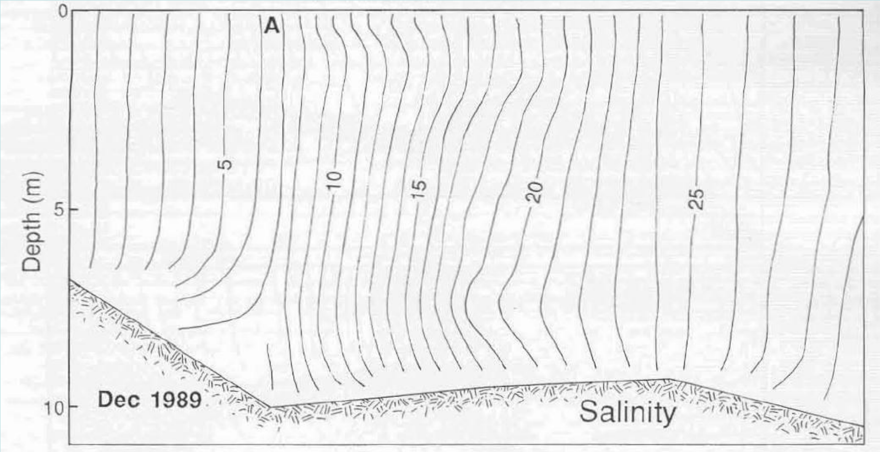

Wolanki et al (1997): long-channel transect in the Far Northern Channel and the corresponding distribution of salinity (ppt) during the spring tide.

Upstream b.c.
Water discharge

Computational mesh

Downstream b.c.
Surface elevation

- Domain length: from Everill Junction to delta front

- The computational mesh is formed by 5551 nodes and 9733 triangular elements.

Assigning bottom elevations

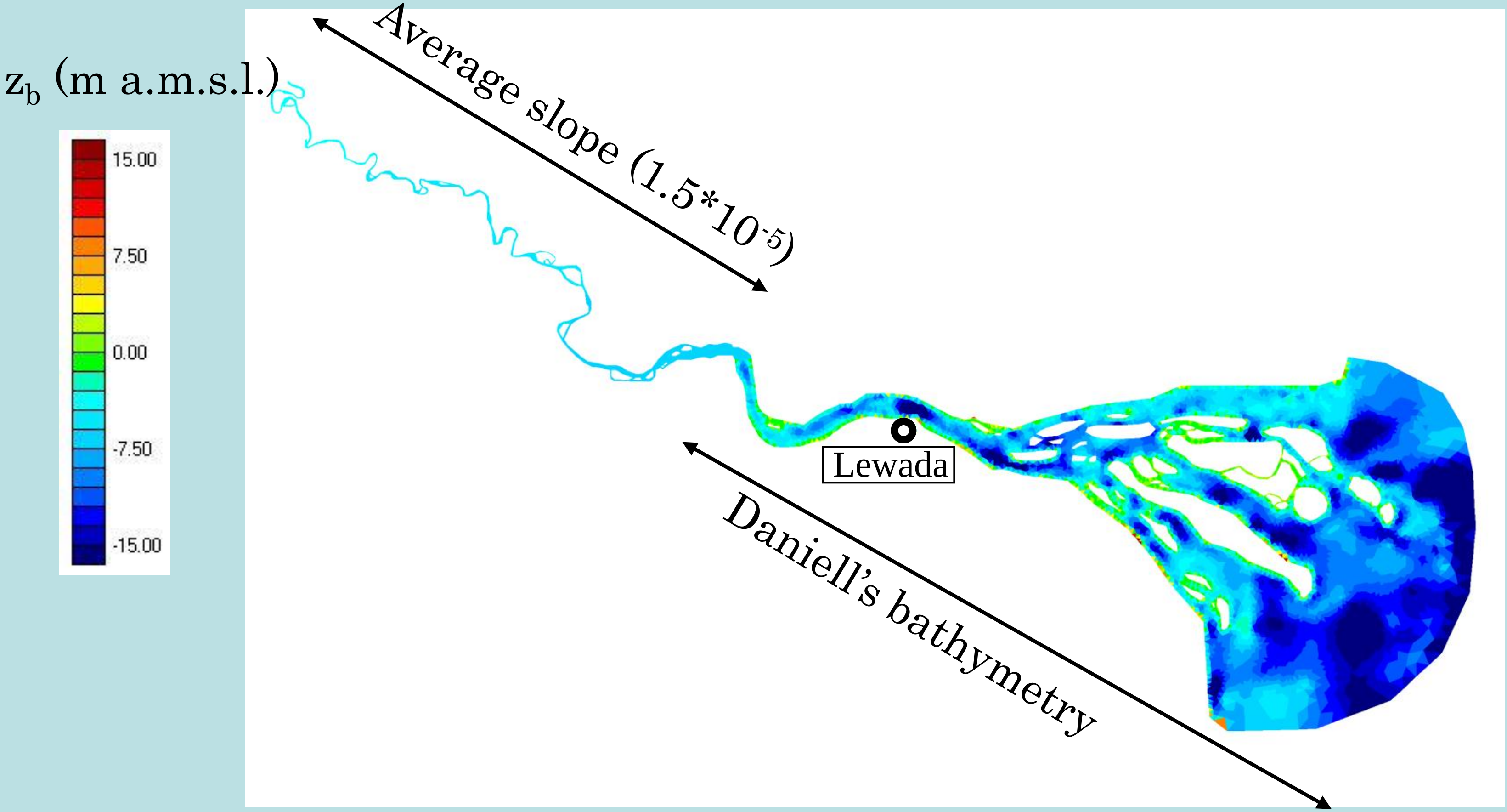

- The bathymetry data of the deltaic part of the river up to 60 km upstream of Lewada are provided by Daniell (2008)

- In the upstream part we use a average slope equal to $1.5*10^{-5}$ (Parker, 2008)

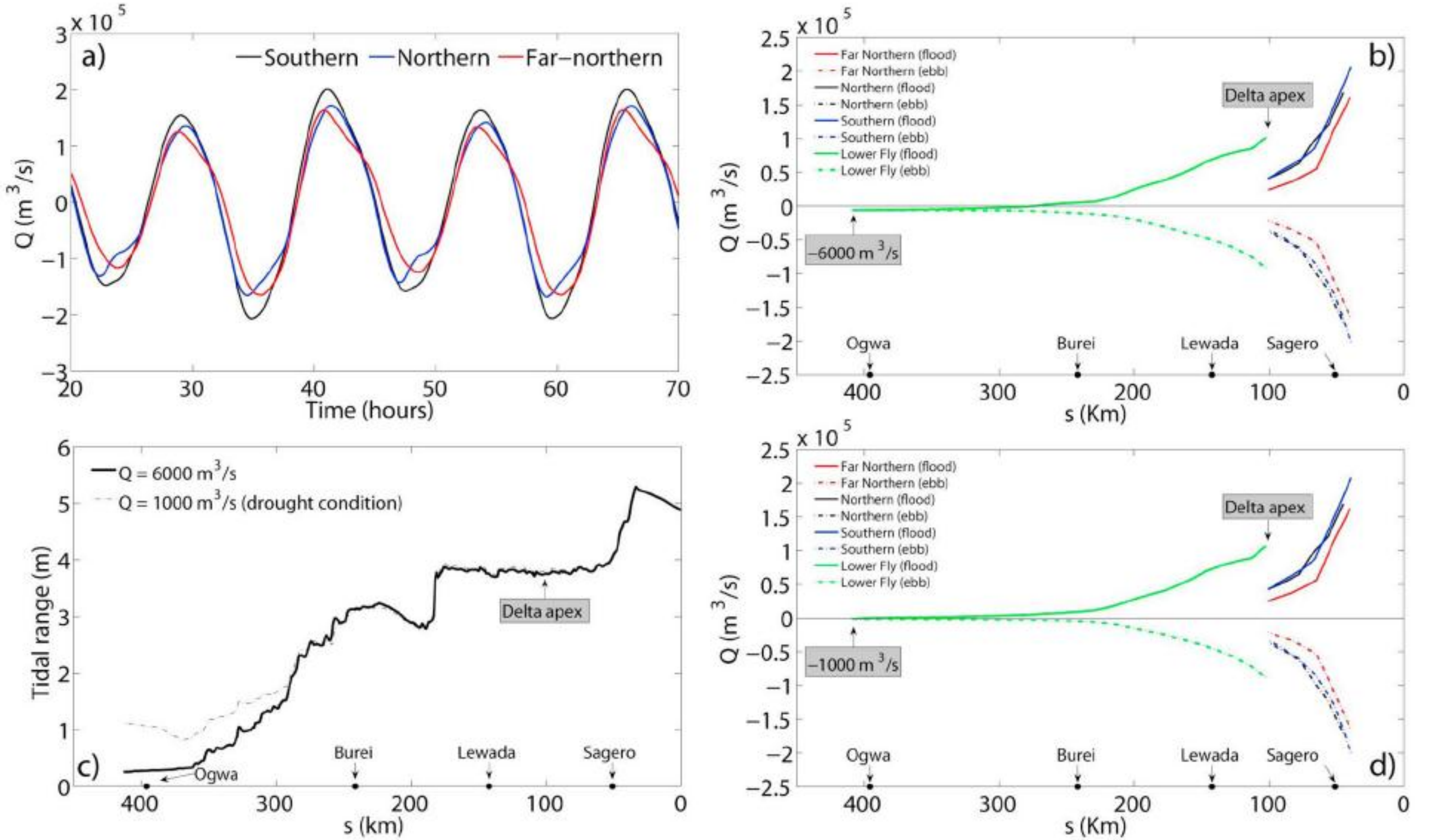

Canestrelli et al., JGR, 2010

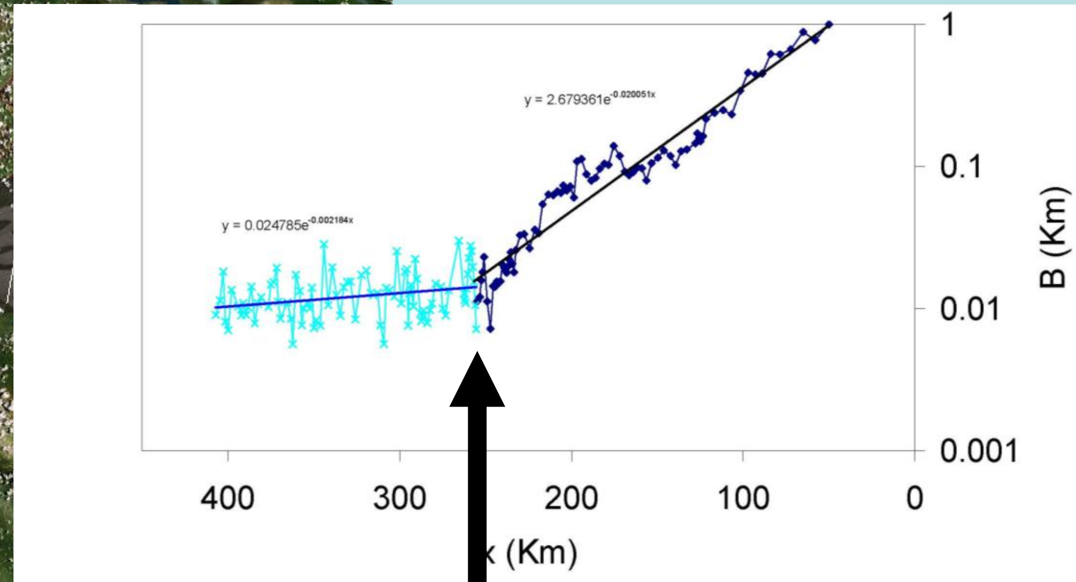

y = 2.679361e-0.020051x
y = 0.024785e-0.002184x
1
0.1
0.01
0.001
B (Km)
400
300
200
100
0
x (Km)

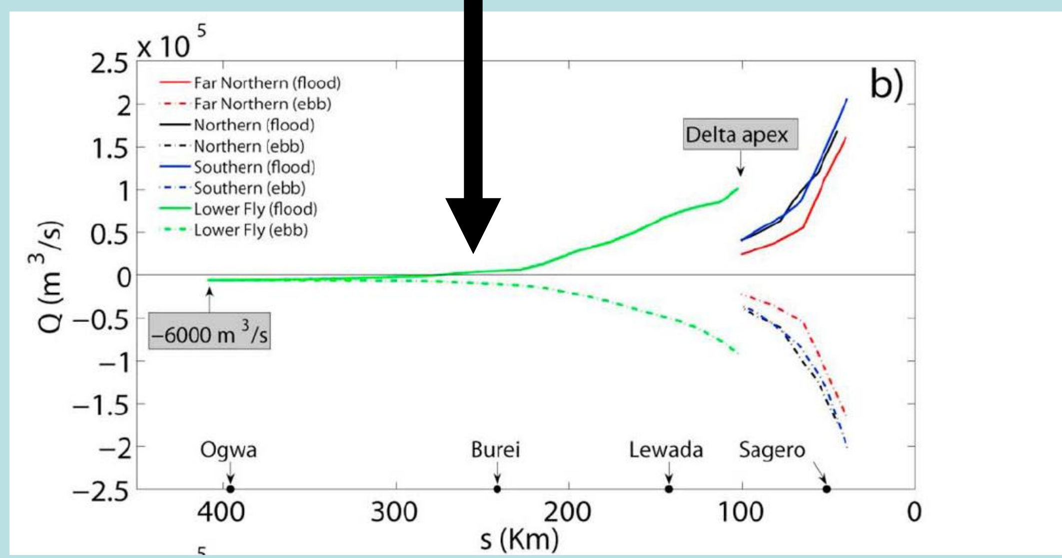

x 10 5
2.5
2
1.5
1
0.5
0
−0.5
−1
−1.5
−2
−2.5
Q (m 3/s)
b)
Far Northern (flood)
Far Northern (ebb)
Northern (flood)
Northern (ebb)
Southern (flood)
Southern (ebb)
Lower Fly (flood)
Lower Fly (ebb)
Delta apex
−6000 m 3/s
Ogwa
Burei
Lewada
Sagero
400
300
200
100
0
s (Km)

Long term bed profile of the estuarine region of the Fly River

Delft3D with two different sediments:

Mud

Wolanski et al., 1995

Ws = 0.1 mm/s in freshwater

Ws = 1 mm/s in salt water

Sand

d=0.1 mm

Simplified geometry

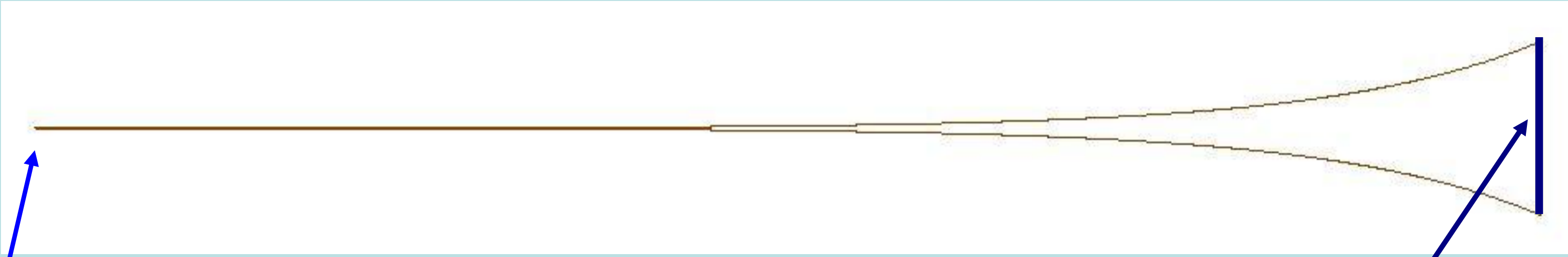

Q = 6000 m^3/s (Wolanski et al., 1997)

C = 0.3 Kg/m^3 (Day et al., 2008, Aalto et al. 2008)

15% sand , 85% mud (Pickup, 1982)

Tide, salinity, equilibrium concentration (mud and sand)

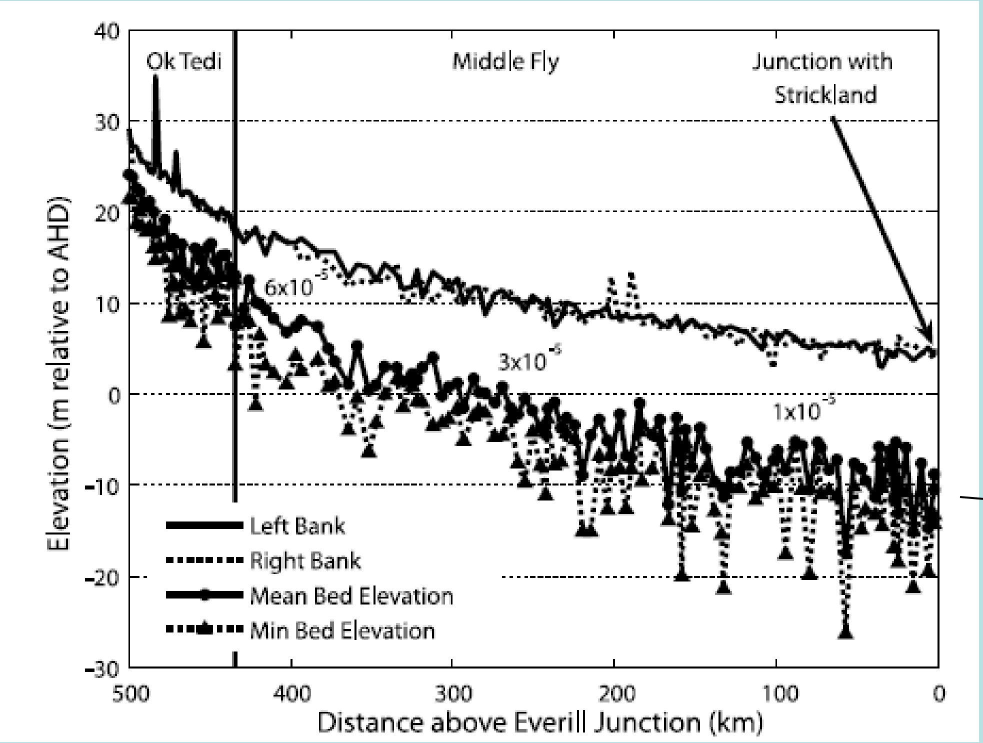

INITIAL CONDITION

LOWER FLY

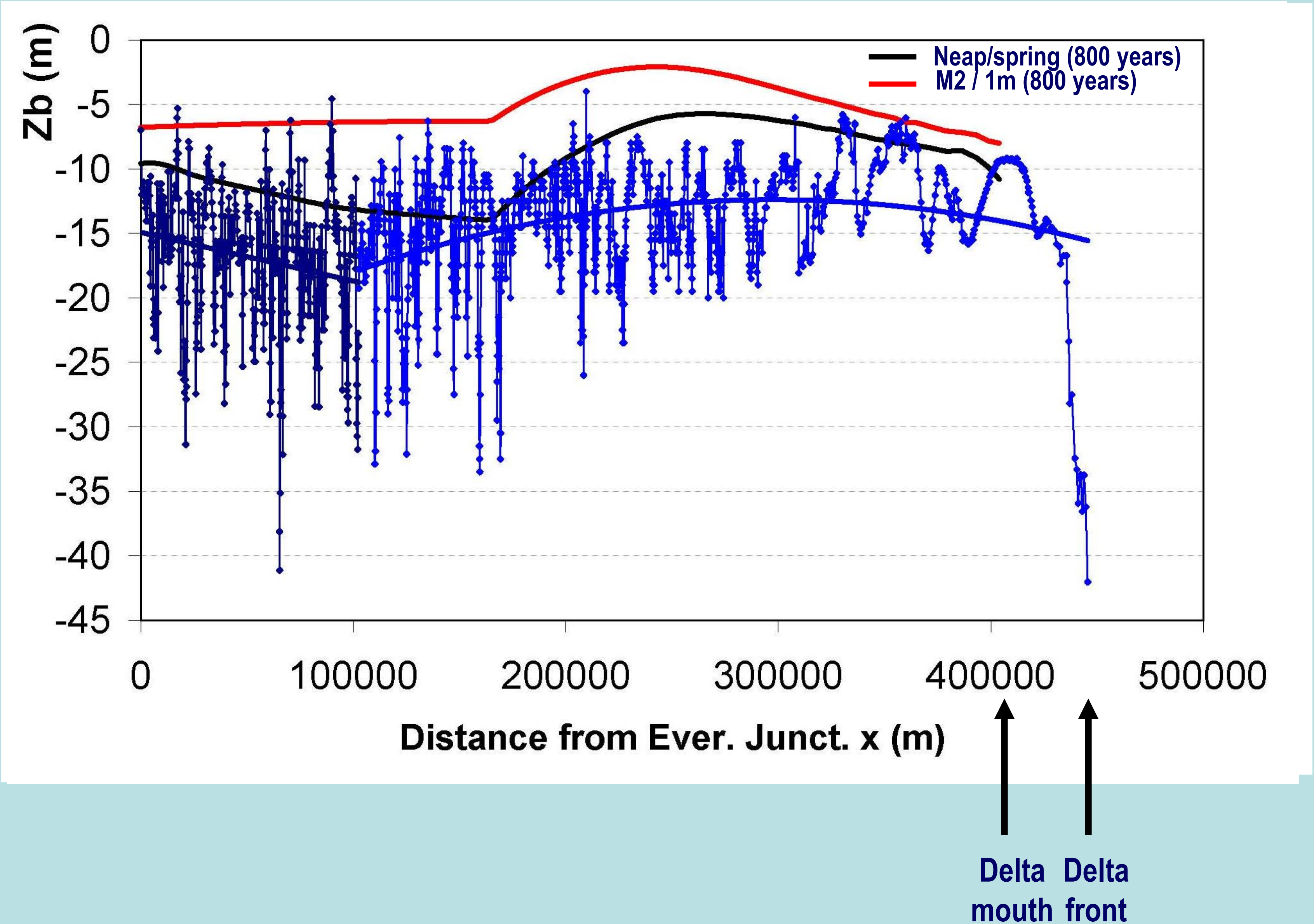

Zb (m)
0
-5
-10
-15
-20
-25
-30
-35
-40
-45
Neap/spring (800 years)
M2 / 1m (800 years)
0
100000
200000
300000
400000
500000
Distance from Ever. Junct. x (m)
Delta mouth
Delta front

CONCLUSIONS

- Simplified models of tidal channels evolution on tidal marshes based on a formative tidal discharge are able to reproduce with a good approximation the statistic of real tidal networks.

- If **long** tidal channels have to be modeled, the complete set of equations should be numerically solved in order to reproduce the detailed bathymetry of the channel.

- When the bottom evolution of an estuary has to be modeled:

  a) a landward monotonic increase of the bed is not observed in general

  b) the concept of <u>maximum discharge = formative discharge</u> cannot be employed in general, since deposition occurring during neap tide largely affect evolution of the bed profile.

- Need of reliable physical based bank erosion models to assess the delicate interplay between vertical and horizontal variations of section.

THANK YOU

FOR YOUR ATTENTION

Bottom elevation in the basin (Tambroni et al. , 2005)

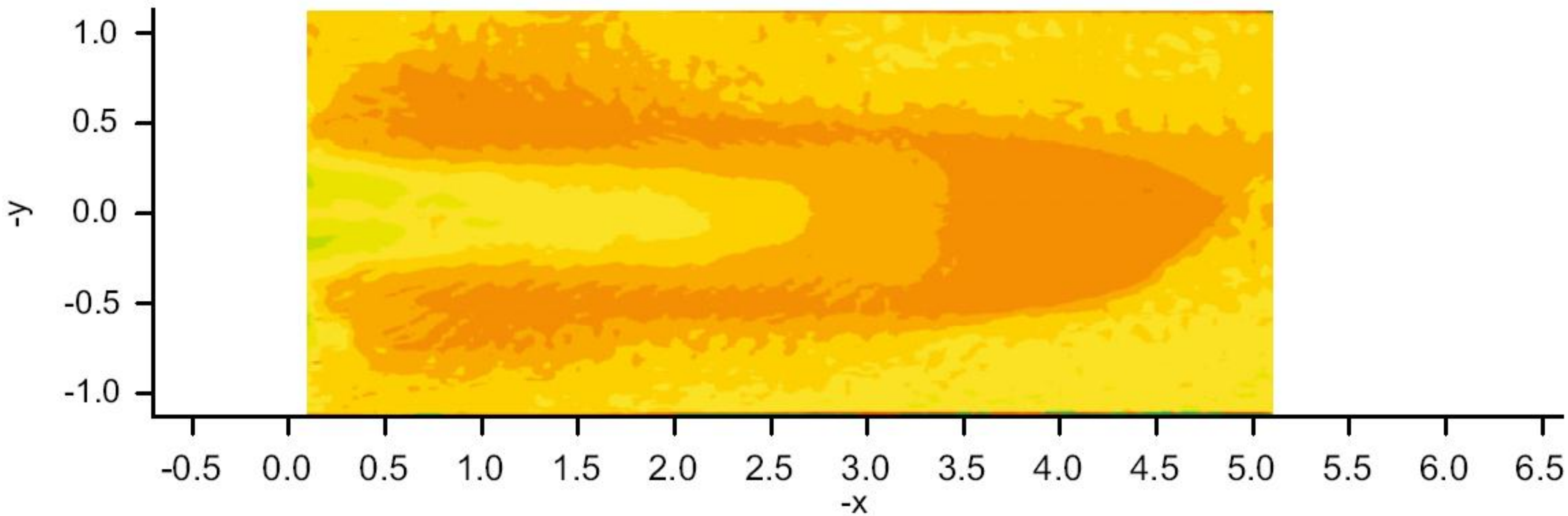

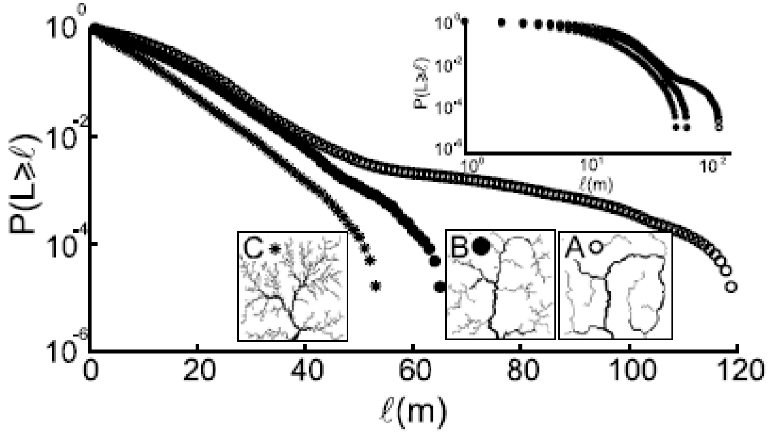

Figure 8. Semilog plot of the exceedance probability of unchanneled length $P(L \geq \ell)$ (versus the current value of length ℓ) computed for the final configurations of the experiments A, B, and C represented in Figure 6. The top inset shows the double logarithmic plot of the exceedance probability of unchanneled length $P(L \geq \ell)$.

$$\boxed{\lambda = \frac{8}{3\pi}\,\frac{U_0}{\chi^2}}$$

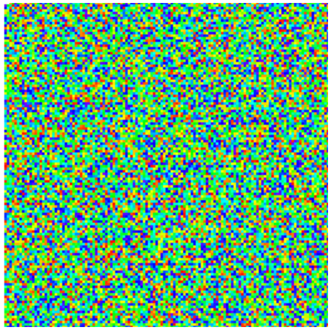

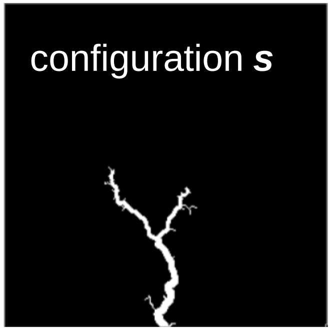

In the case of fluvial settings: **Rinaldo et al., *Phys. Rev. Lett.*, 1993; Rigon et al., *JGR*, 1994; Rinaldo et al., *Nature*, 1995**

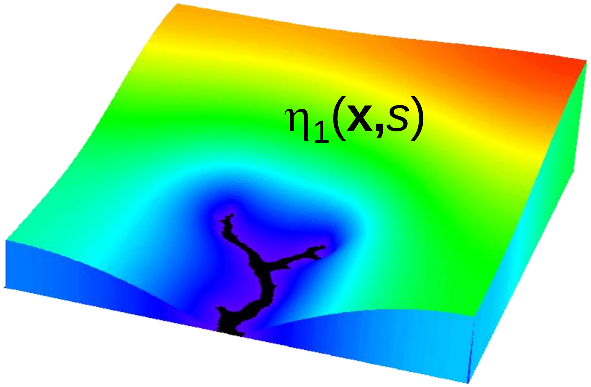

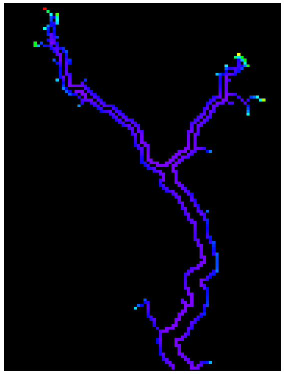

Physical settings, temperature T, threshold $\tau_c \ldots \tau_c(x)$, geometry

For a given configuration ***s***:

$\eta_1(\mathbf{x},s)$, drainage directions, contributing areas, $E(s)=<\eta_1(\mathbf{x},s)>$, $P(s) \propto \exp(-E(s)/T)$

$\tau(\mathbf{x},s)$ on the neighbors of the channel network

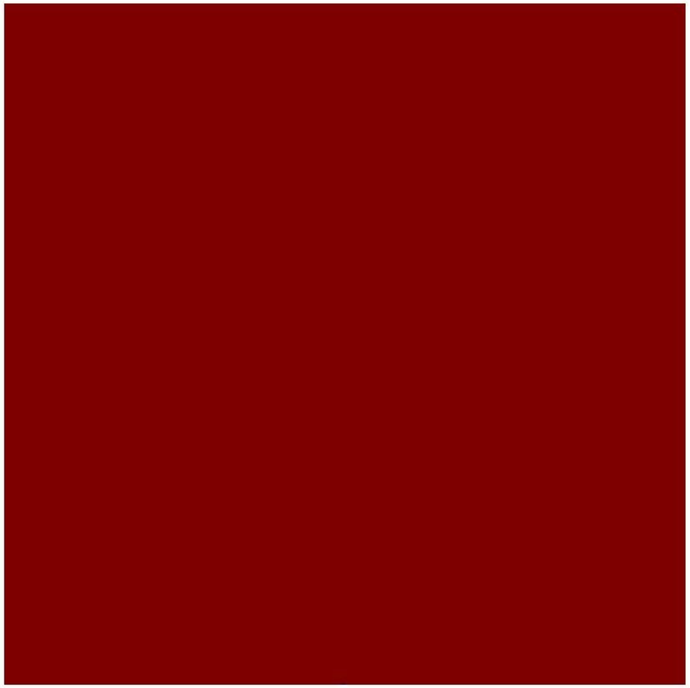

Threshold exceedences $[\tau(\mathbf{x},s)-\tau_c>0]$ are computed and ranked

$[\tau(x,s)-\tau_c>0]_1$
$[\tau(x,s)-\tau_c>0]_2$
....
$[\tau(x,s)-\tau_c>0]_K$
....
$[\tau(x,s)-\tau_c>0]_N$

A new pixel is “somehow”selected to become a part of the network

B is computed ($\Omega \propto kA$; β=B/D=cost)

a width is assigned to network cross sections and a new configuration ***s'*** is determined

LOCAL VALUE OF THE BOTTOM SHEAR STRESS

$$\tau(\mathbf{x}) = \rho g \left[\eta_0 + \eta_1(\mathbf{x}) - z(\mathbf{x})\right] \nabla \eta_1(\mathbf{x})$$

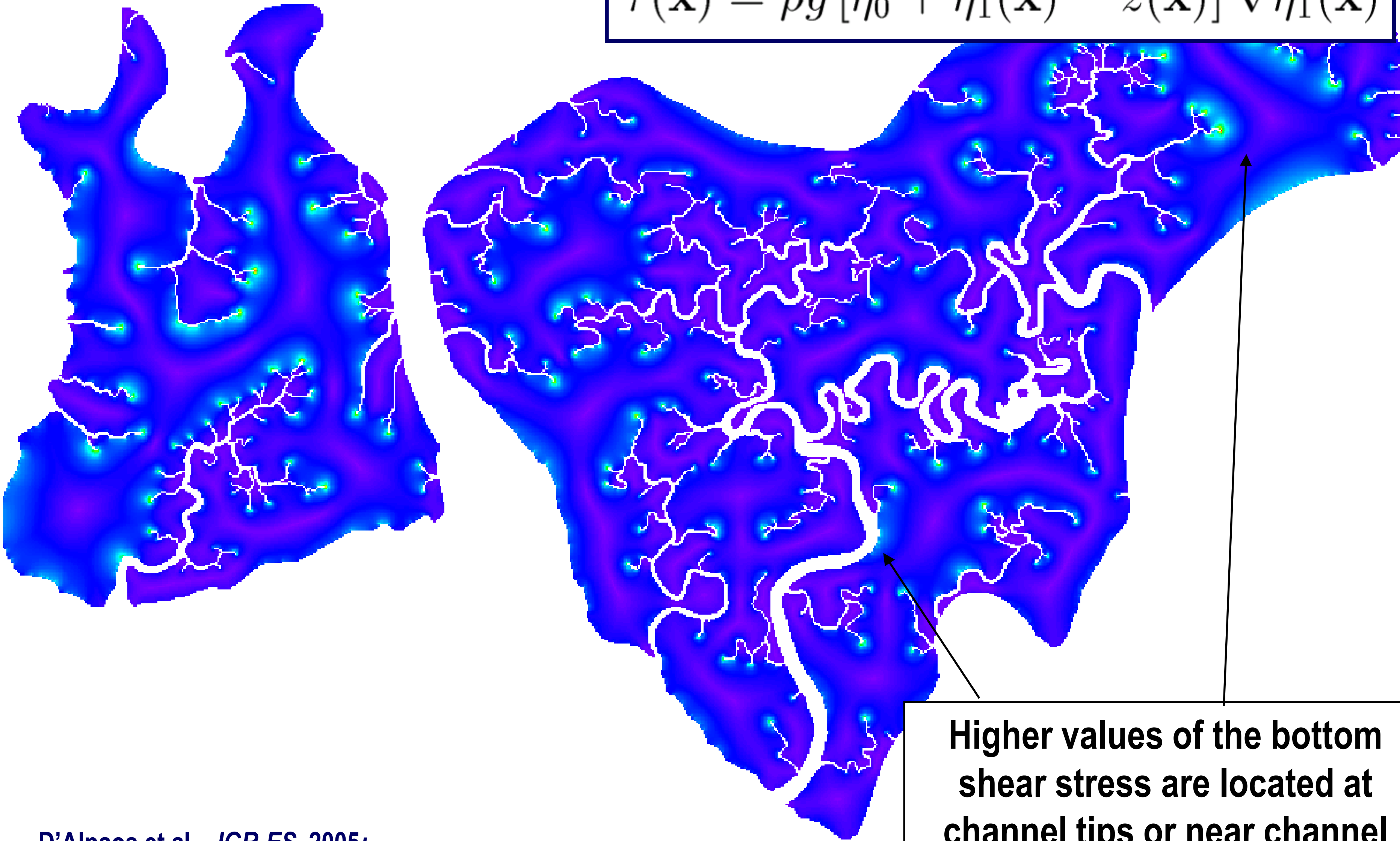

Higher values of the bottom shear stress are located at channel tips or near channel bends

D'Alpaos et al., *JGR-ES*, 2005;
Feola et al., *WRR*, 2005

HEADWARD GROWTH CHARACTER of NETWORK DEVELOPMENT

Hughes et al,. *GRL* 2009

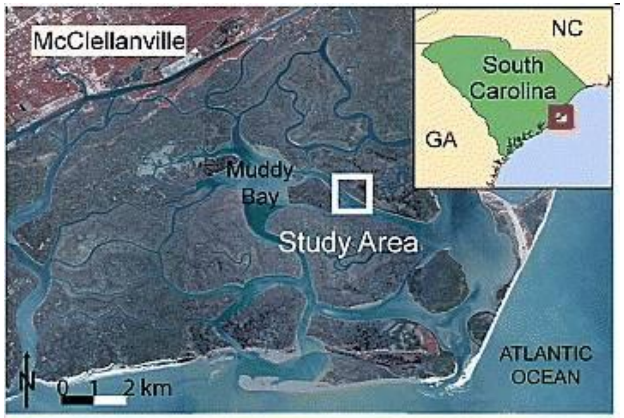

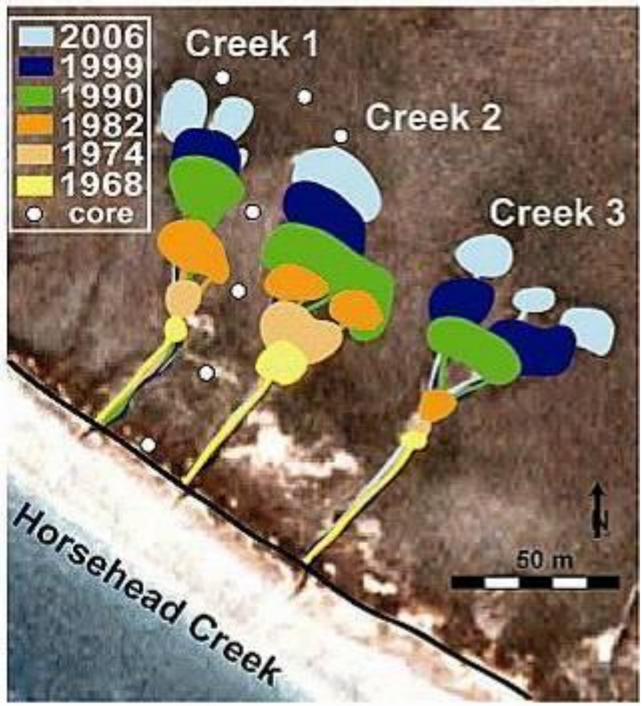

(e.g. Steers, 1960; Pestrong, 1965; French and Stoddart, 1992; Collins et al. 1987; Wallace et al. 2005; D'Alpaos et al., 2007)

O'BRIEN-JARRETT-MARCHI LAW

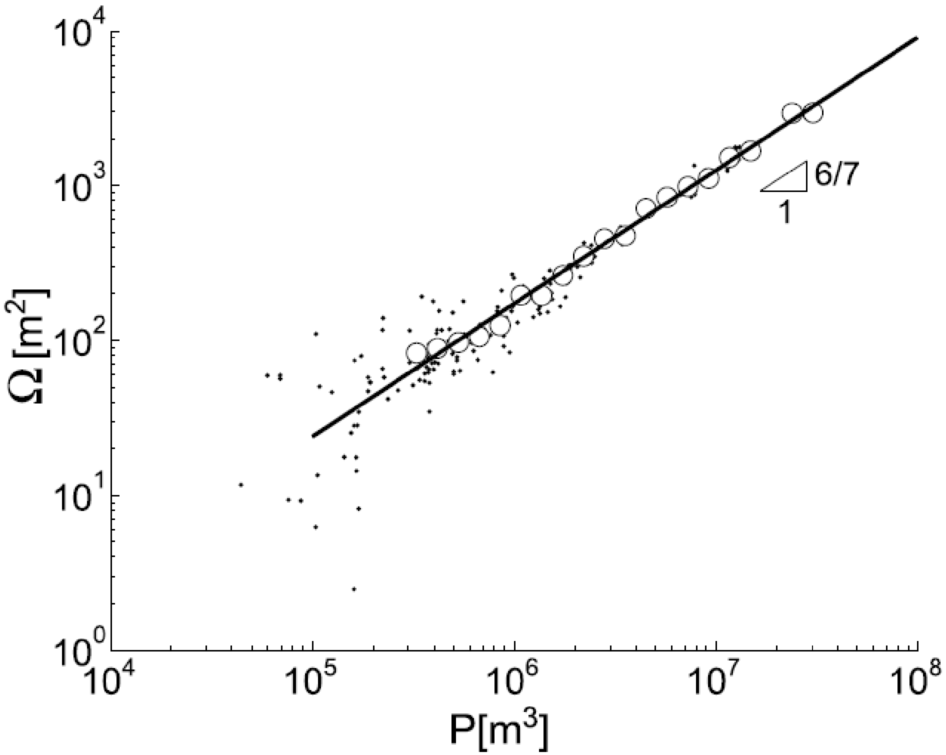

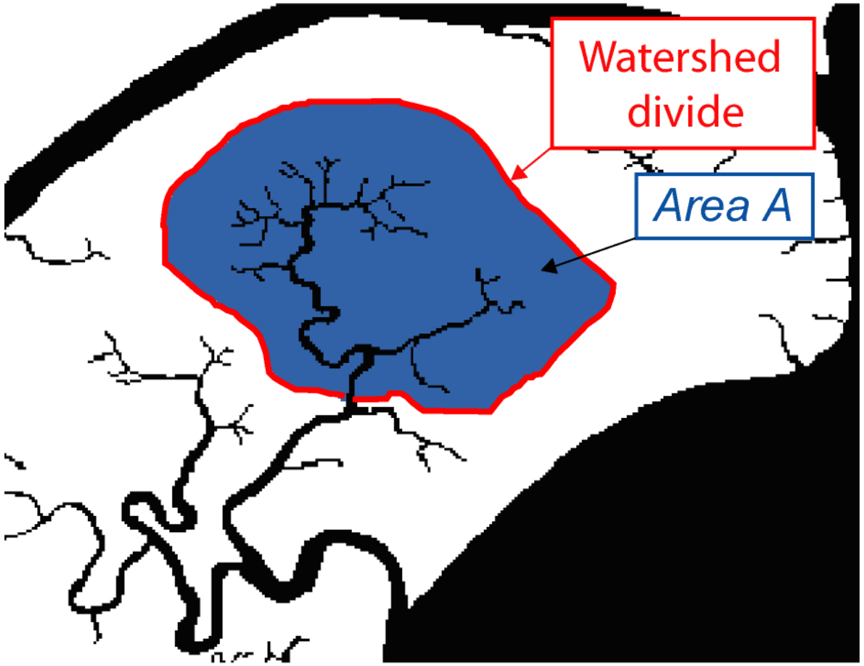

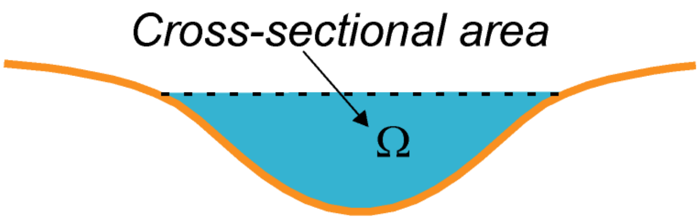

$$\boxed{\Omega \propto Q_{max}}$$

Myrick & Leopold, 1963;
Rinaldo et al., 1999

$$\boxed{\Omega = k\ P^{\alpha}}$$

O'Brien, 1969; Jarrett, 1976; Marchi 1990;
D'Alpaos et al., *Rendiconti Lincei*, 2009;
D'Alpaos et al., *JGR* 2010

EVOLUTION OF A TIDAL CHANNEL FLANKED BY TIDAL FLATS

We neglect:

-presence of vegetation

-resuspension of sediment by wind wave motion

3-D view

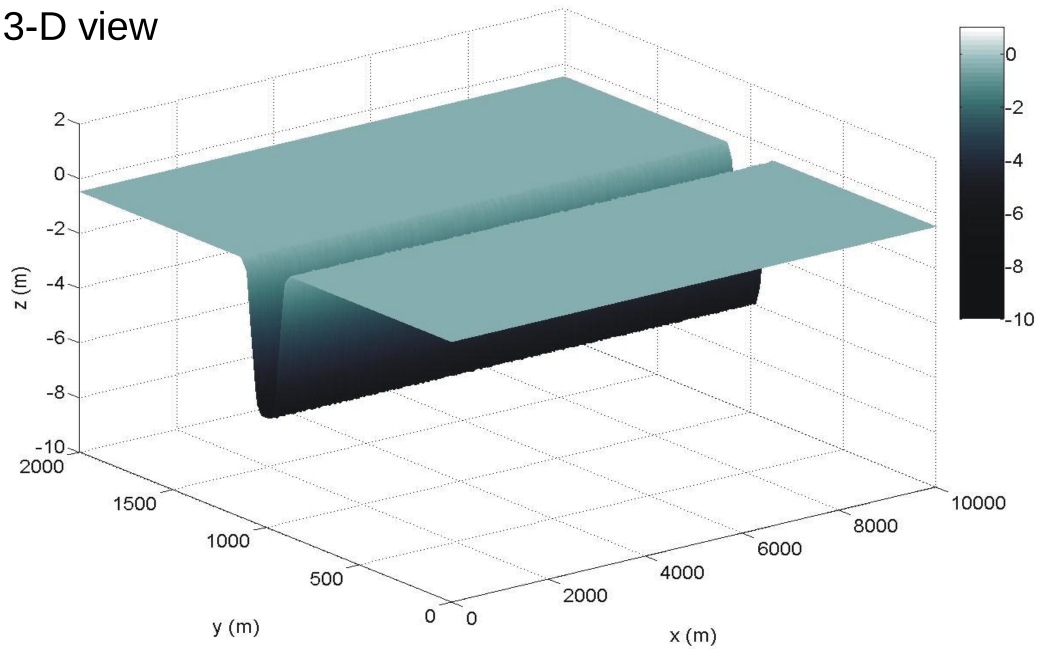

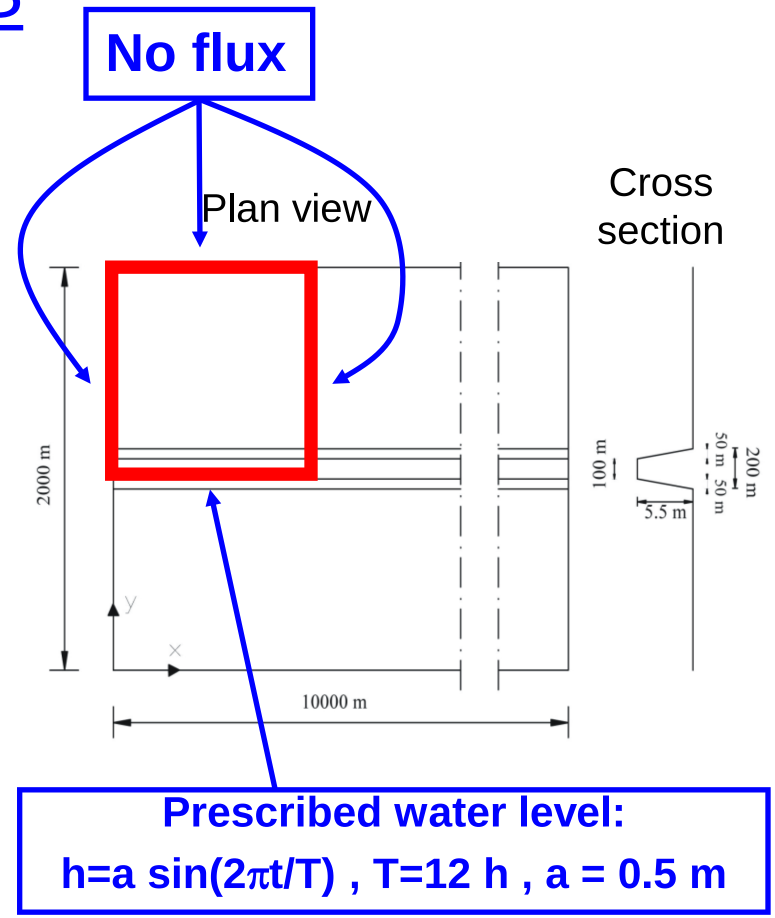

Smaller part of the domain (1500 m long) ⇨ **We neglect tide propagation within the main channel**

Parameters:

K_s=30 $m^{1/3}s^{-1}$; d_s=0.05 mm (uniform sand) ; a_r=0.3 m (height of bottom irregularities-subgrid model)

Cell resolution varies gradually from 10 m into the channel to 30 m at the boundary of the tidal flats.

Neglecting tide propagation within the channel

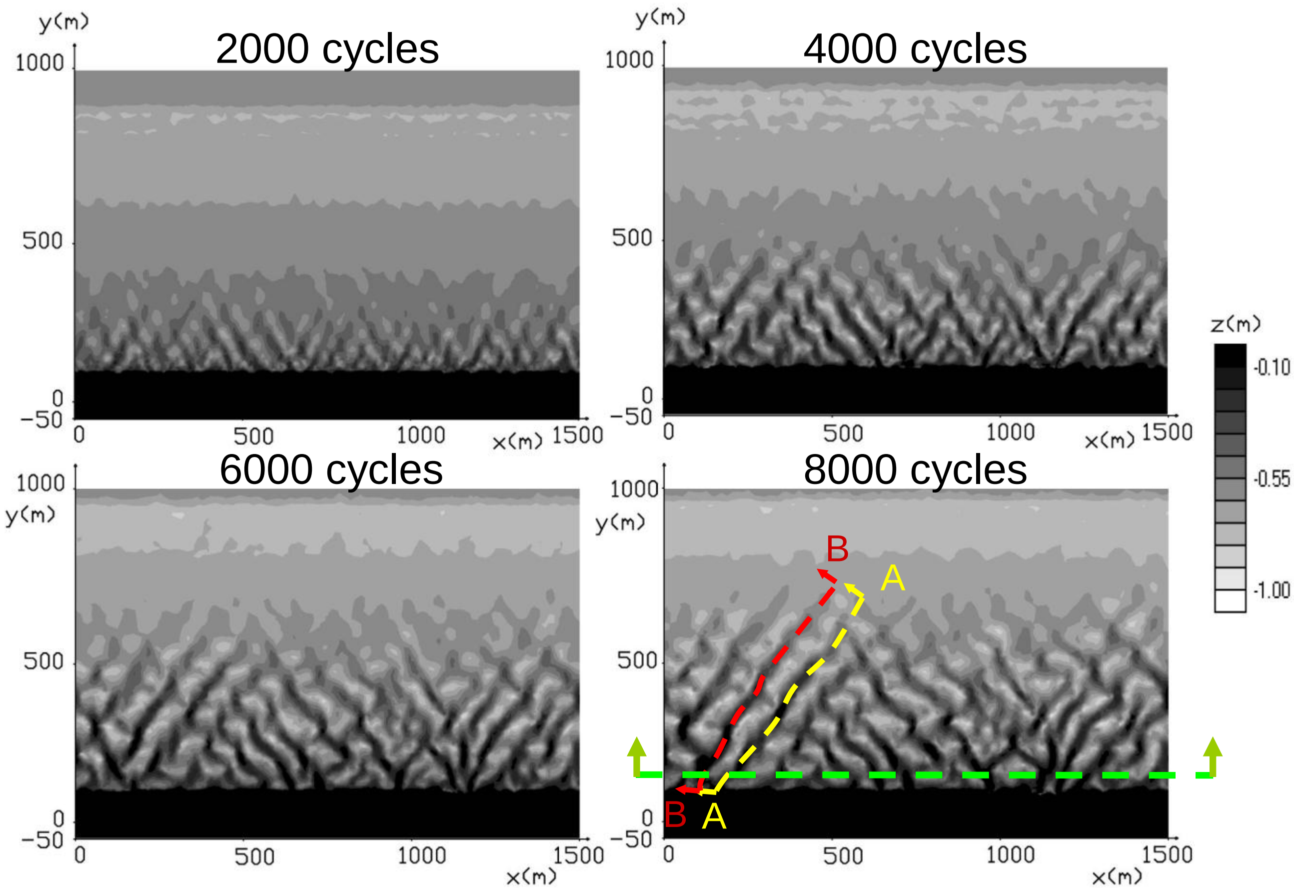

– Tidal flat is progressively dissected by creeks, which tend to dispose at an angle of about ±60° with respect to the direction of the main channel axis.

Section A-A:

Section B-B:

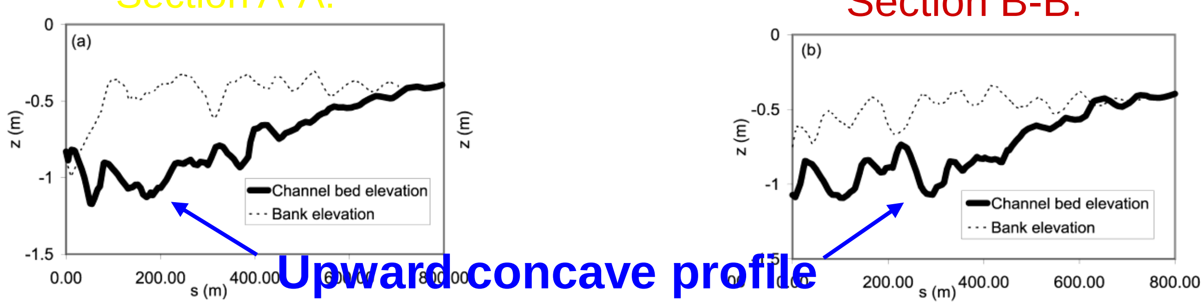

Spacing between the tidal flat creeks. Two peaks: 115 m and 83 m.

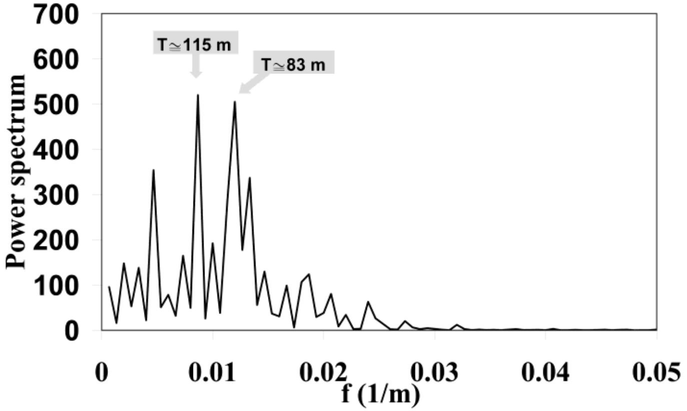

A possible mechanism that can favour the inception of tidal flats channelization is:

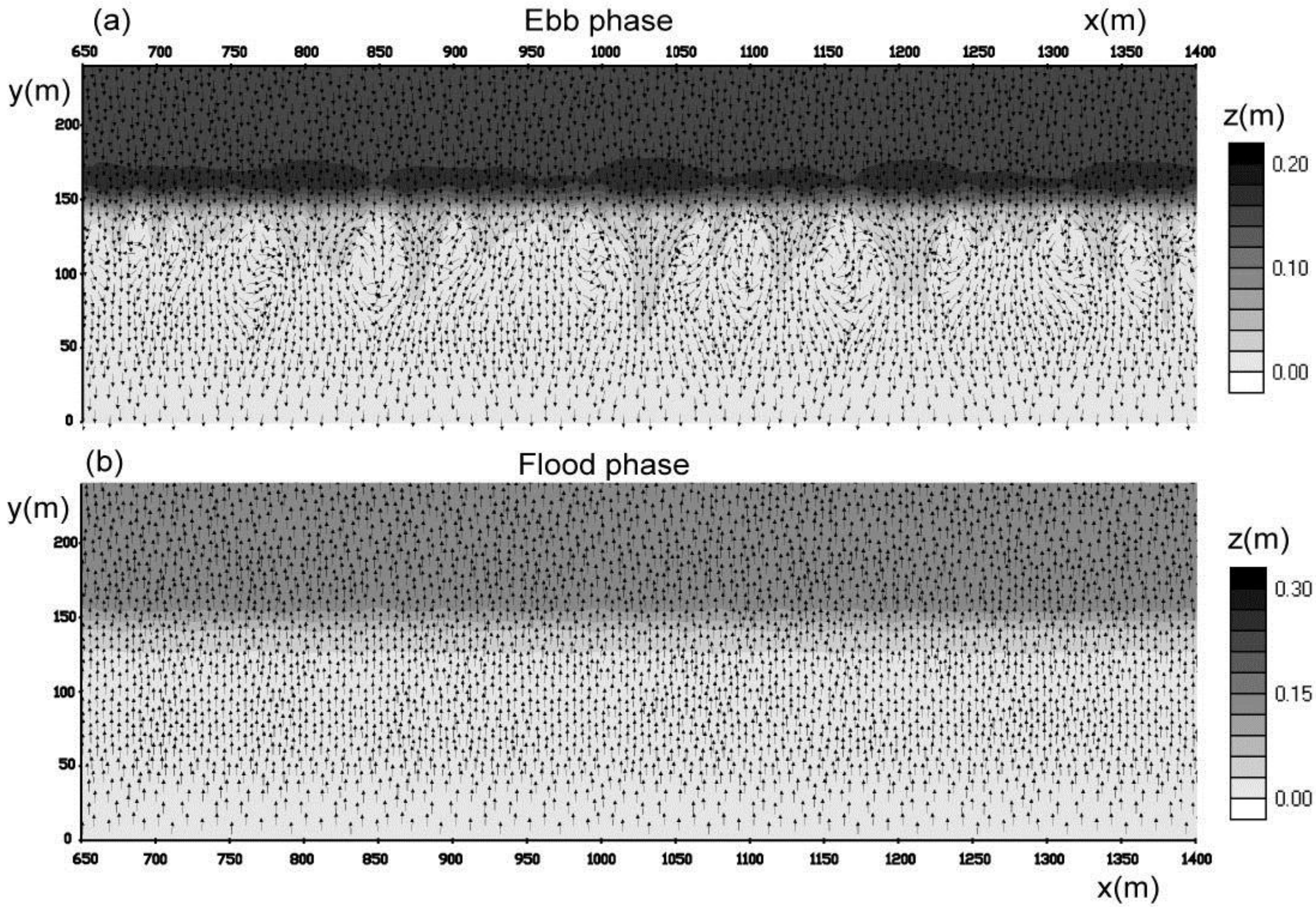

<u>Confronto con i canali lagunari: Canale Melison (1901)</u>

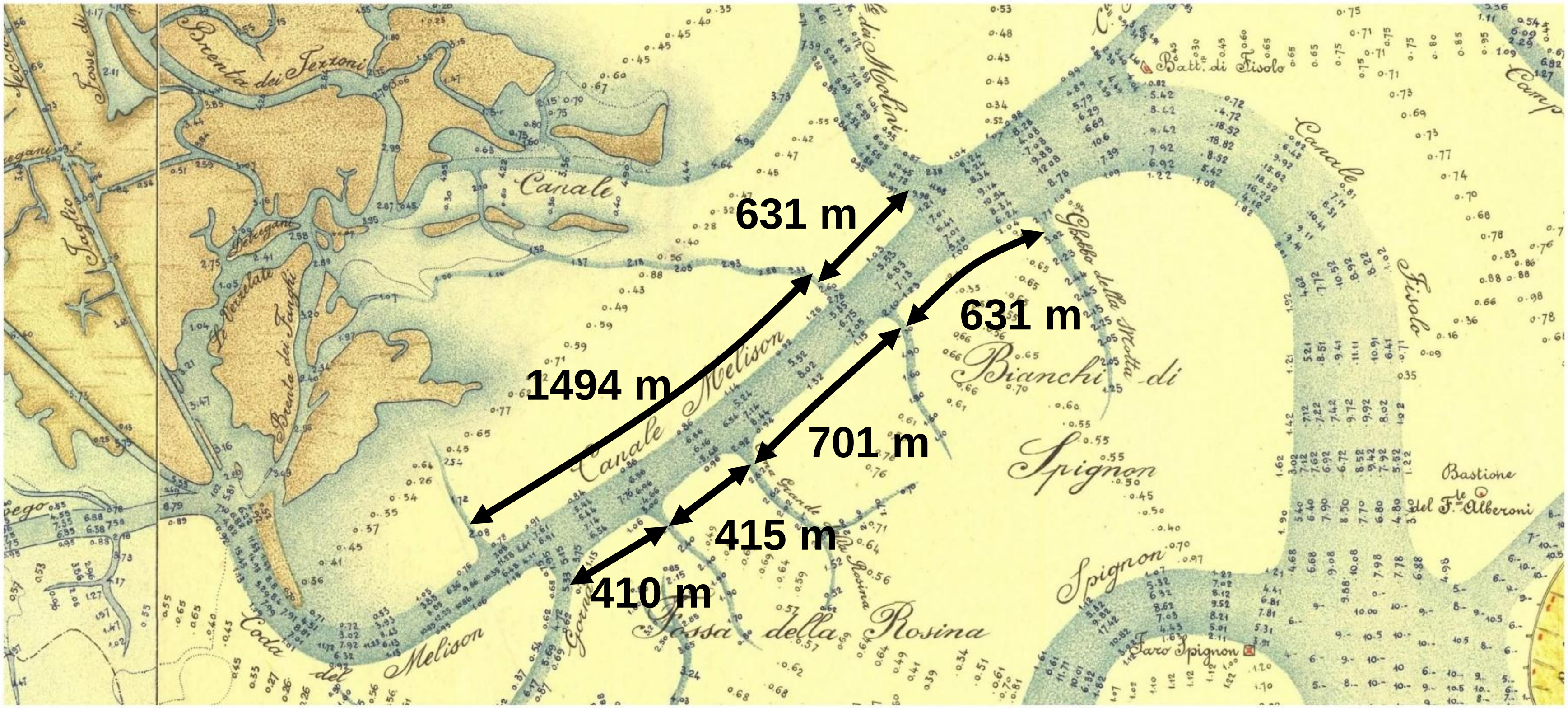

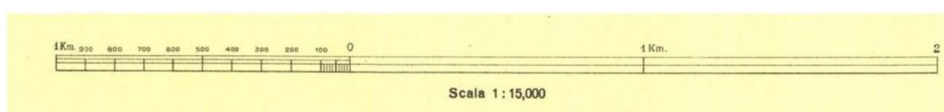

Confronto con i canali lagunari: Canale del Cornio (1901)

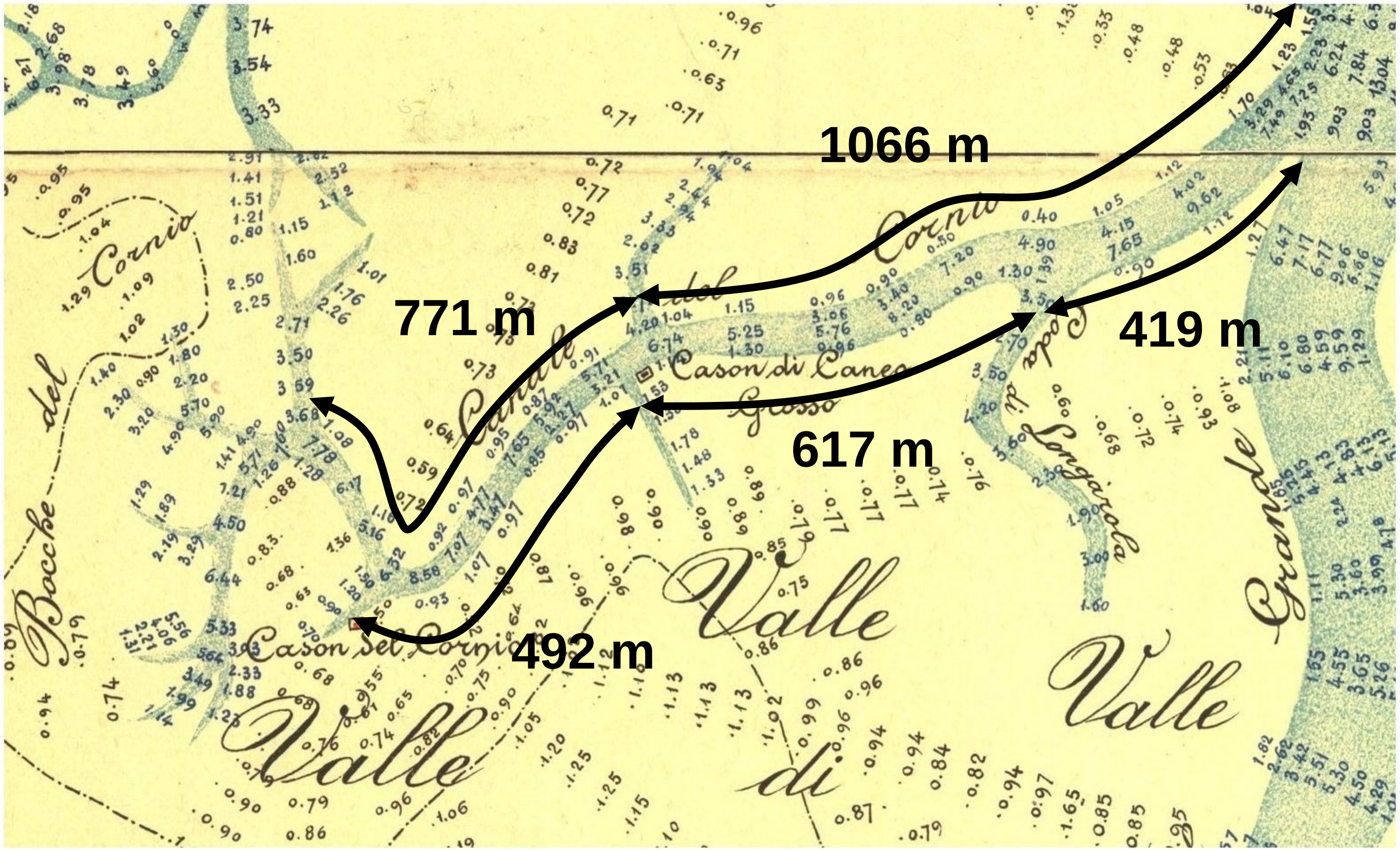

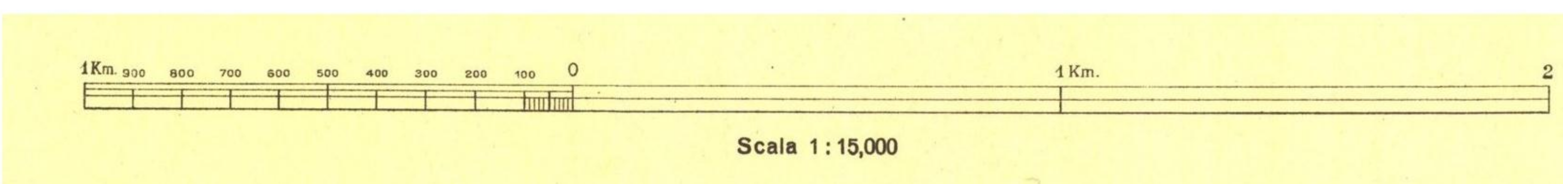

Confronto con i canali lagunari: Canale Lombardo (1901)

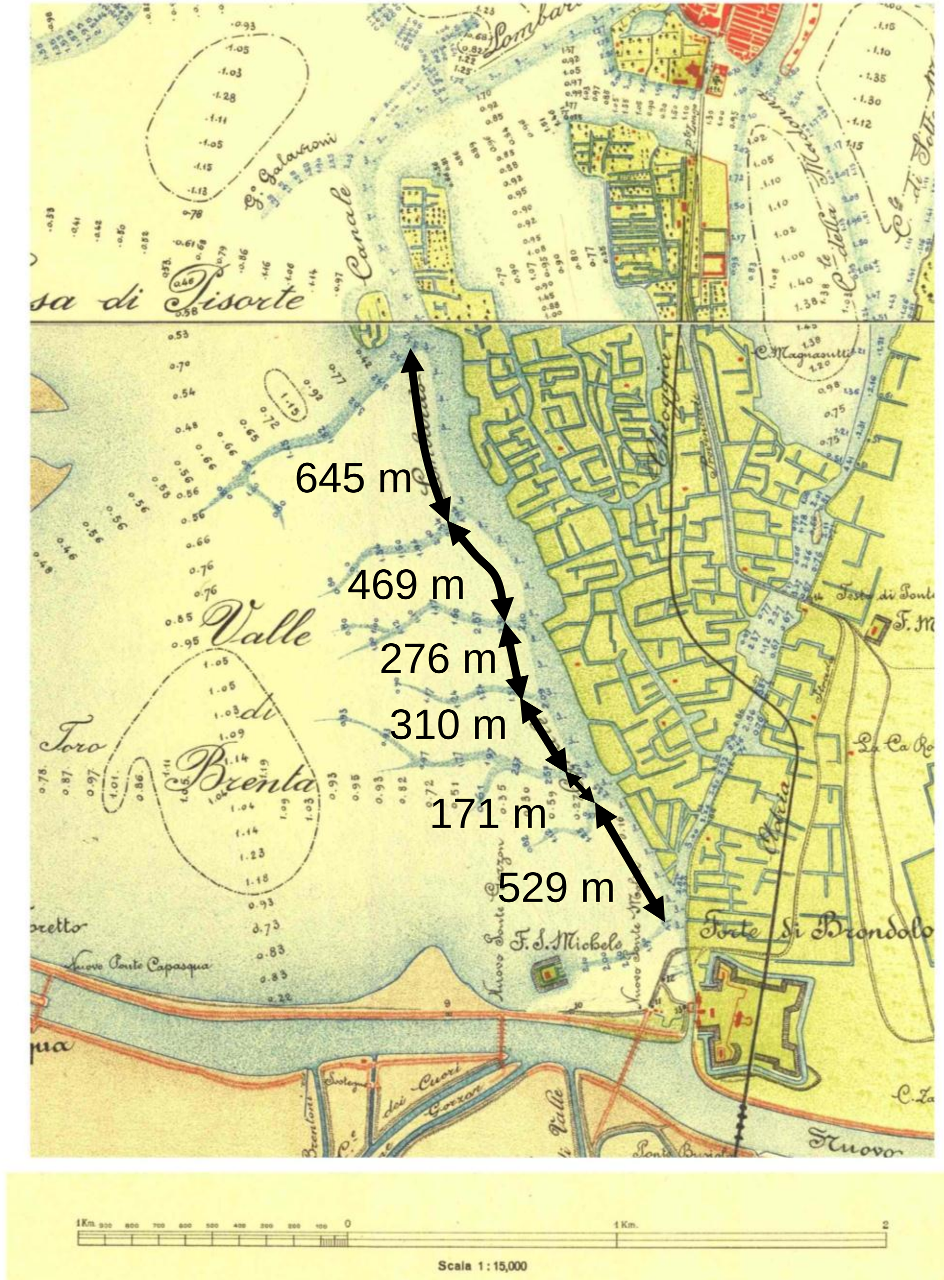

MODEL CALIBRATION

	Sagero River Junction	Lewada		Burei Junction		Ogwa	
River Distance (km)	0	95		112		370	
		Num	Obs	Num	Obs	Num	Obs
River Lag MHWS (hrs)	0	3.1	3.0	5.6	5.5	12.5	12.3
River Lag MLWS (hrs)	0	4.3	4.5	7.2	7.0	13.4	13.5
Range Ratio %	100	94	97	81	83	8	9

SMEC navigation charts.

Delta: $\boxed{K_s = 65\ m^{1/3}s^{-1}}$

Wolanski (1998) : $K_s = 67\ m^{1/3}s^{-1}$

River: $K_s = 45\ m^{1/3}s^{-1}$

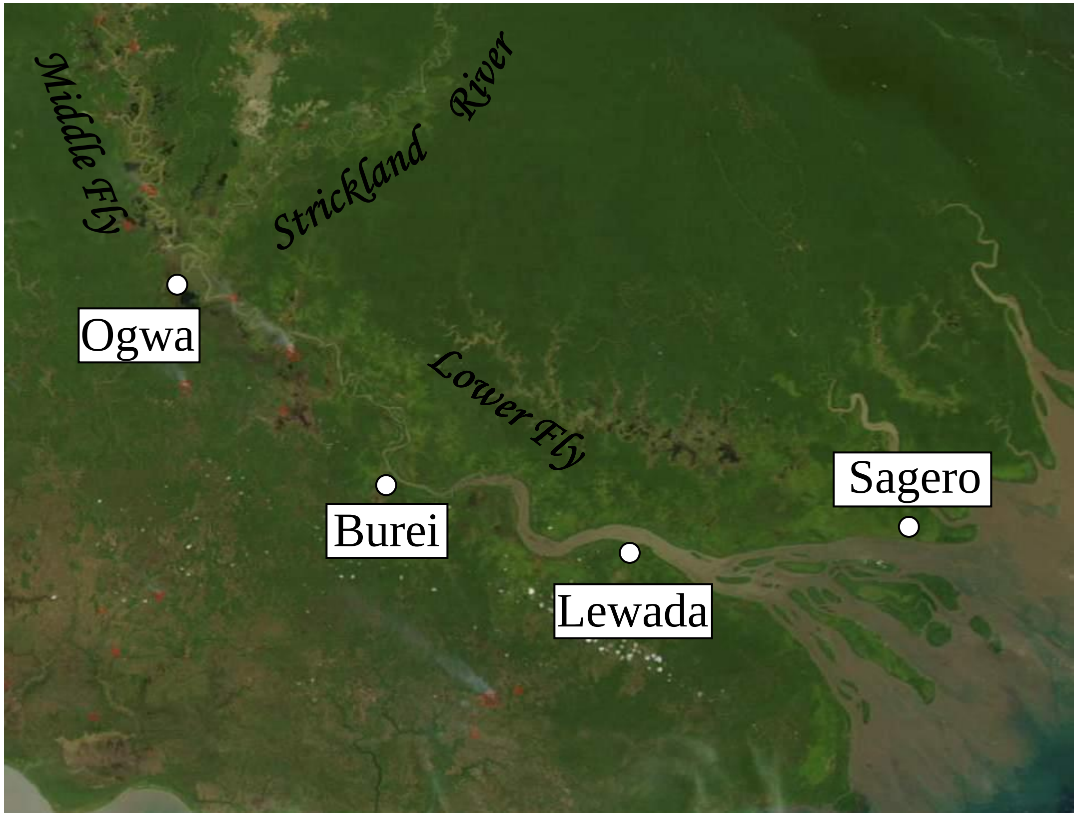

Water discharge at the distributary mouths

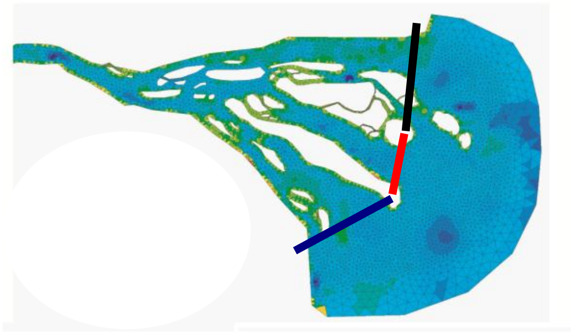

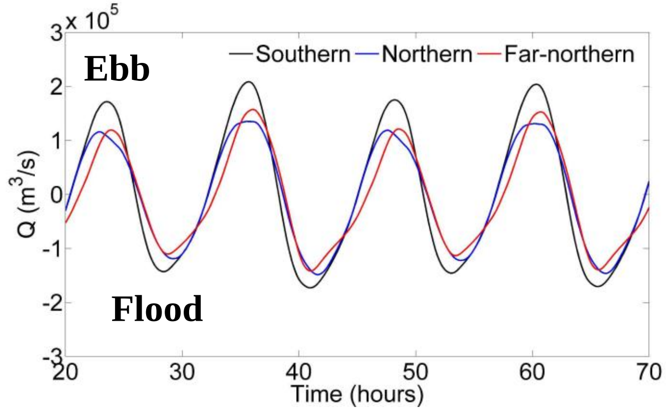

water discharge at distributary mouths >> riverine discharge

Maximum shear stress distribution

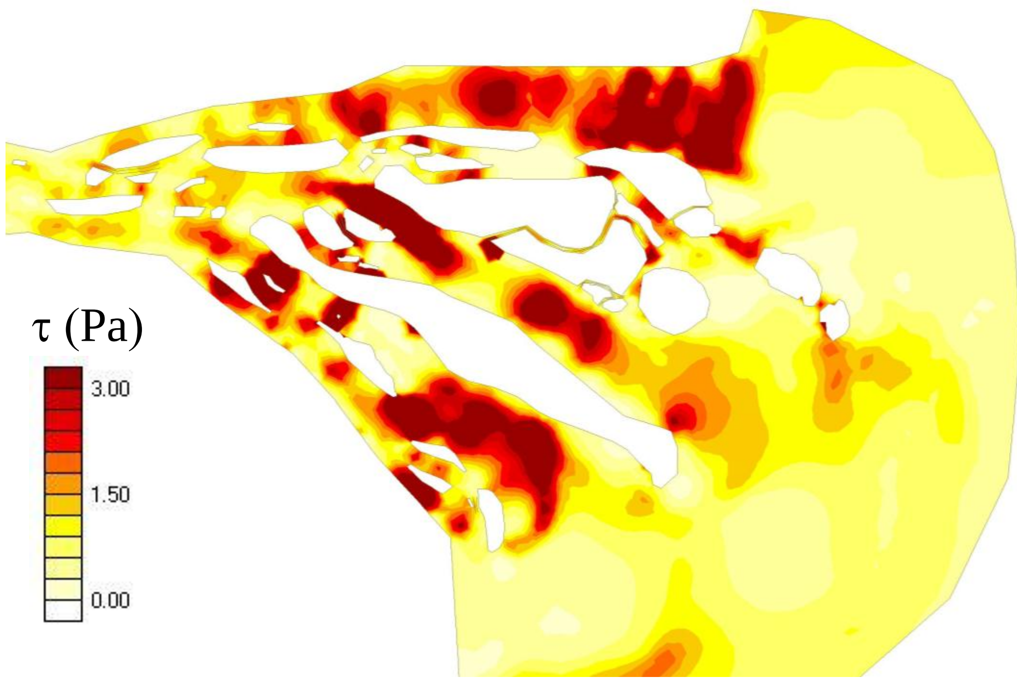

- While wave energy reaches maximum values on the delta front and quickly decreases landward into the distributary channels, the tidal energy is small on the delta front and increases in the distributary channels ➤ it shapes the islands and the channels.

Flood and ebb dominance

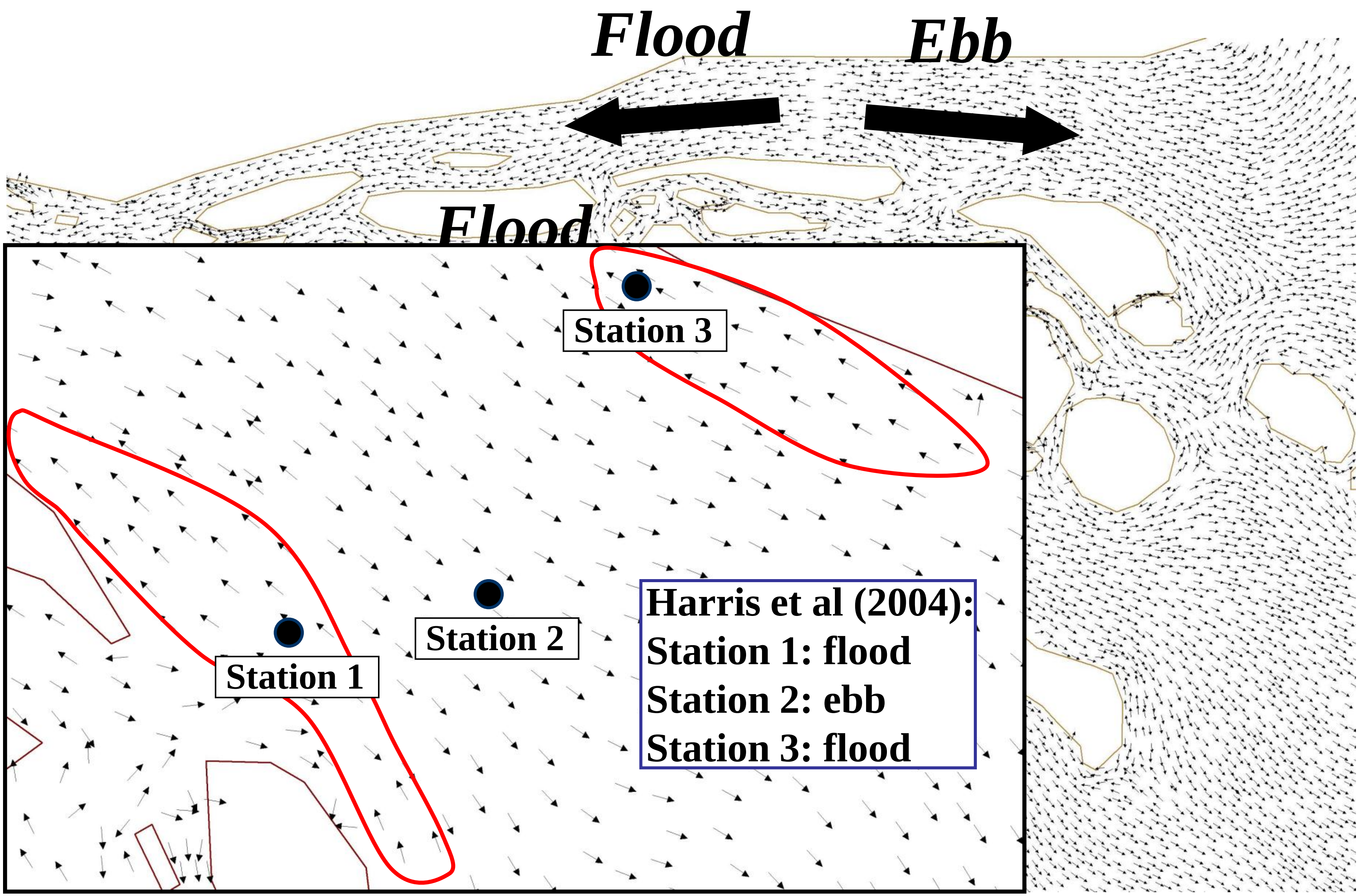

Comparison between model result and Canale del bari bed profile

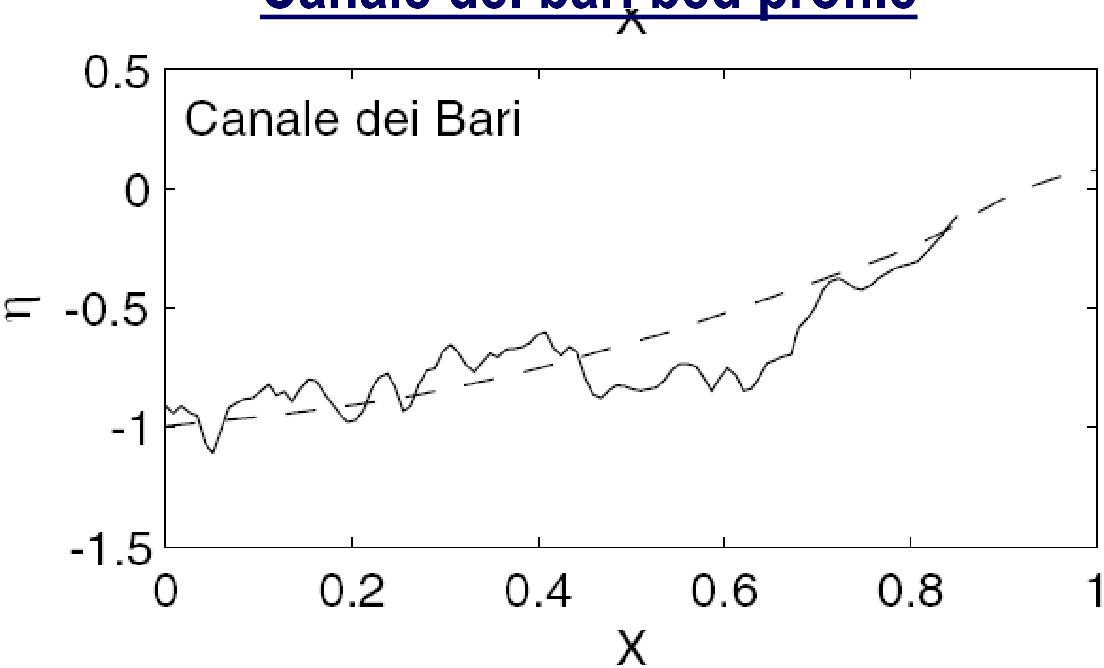

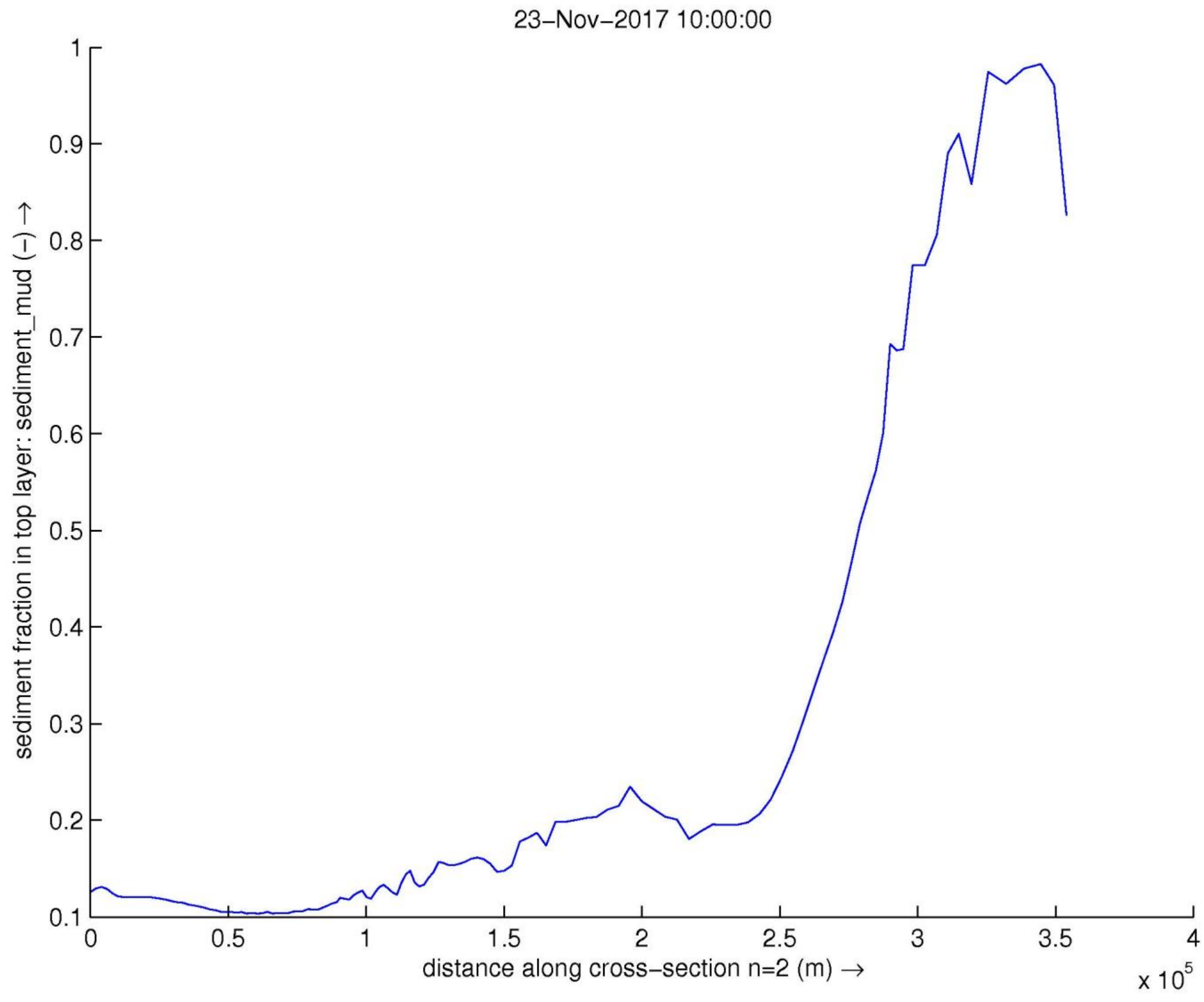

23−Nov−2017 10:00:00
sediment fraction in top layer: sediment_mud (−) →
distance along cross−section n=2 (m) →
x 10^5
0
0.5
1
1.5
2
2.5
3
3.5
4
0.1
0.2
0.3
0.4
0.5
0.6
0.7
0.8
0.9
1

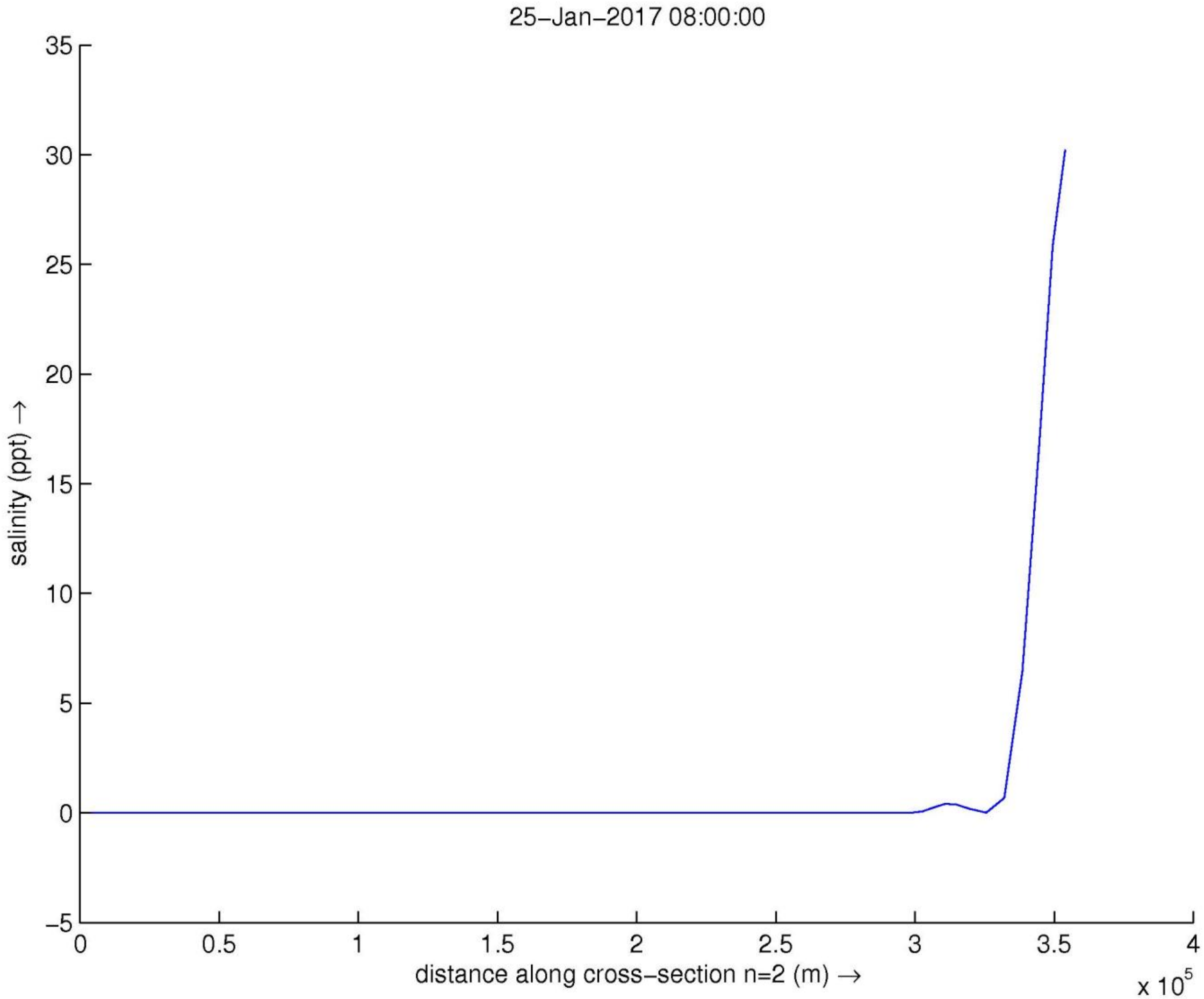
25−Jan−2017 08:00:00
salinity (ppt) →
35
30
25
20
15
10
5
0
−5
0
0.5
1
1.5
2
2.5
3
3.5
4
distance along cross−section n=2 (m) →
x 10^5